The interferon-regulated host factor hnRNPA0 modulates HIV-1 production by interference with LTR activity, mRNA trafficking, and programmed ribosomal frameshifting

Fabian Roesmann,[1] Helene Sertznig,[2] Katleen Klaassen,[1] Alexander Wilhelm,[1] Delia Heininger,[1] Stefanie Heß,[1] Carina Elsner,[2] Rolf Marschalek,[3] Mario L. Santiago,[4] Stefan Esser,[5,6] Kathrin Sutter,[2,5] Ulf Dittmer,[2,5] Marek Widera[1]

AUTHOR AFFILIATIONS See affiliation list on p. 20.

ABSTRACT The interplay between host factors and viral components impacts viral replication efficiency profoundly. Members of the cellular heterogeneous nuclear ribonucleoprotein family (hnRNPs) have been extensively studied as HIV-1 host dependency factors, but whether they play a role in innate immunity is currently unknown. This study aimed to identify hnRNPA0 as a type I interferon (IFN)-repressed host factor in HIV-1-infected cells. Knockdown of hnRNPA0, a situation that mirrors conditions under IFN stimulation, increased LTR activity, export of unspliced HIV-1 mRNA, viral particle production, and thus, increased infectivity. Conversely, hnRNPA0 overexpression primarily reduced plasmid-driven and integrated HIV-1 long terminal repeat (LTR) activity, significantly decreasing total viral mRNA and protein levels. In addition, high levels of hnRNPA0 significantly reduced the HIV-1 programmed ribosomal frameshifting efficiency, resulting in a shift in the HIV-1 p55/p15 ratio. The HIV-1 alternative splice site usage remained largely unaffected by altered hnRNPA0 levels suggesting that the synergistic inhibition of the LTR activity and viral mRNA transcription, as well as impaired ribosomal frameshifting efficiency, are critical factors for efficient HIV-1 replication regulated by hnRNPA0. The pleiotropic dose-dependent effects under high or low hnRNPA0 levels were further confirmed in HIV-1-infected Jurkat cells. Finally, our study revealed that hnRNPA0 levels in PBMCs were lower in therapy-naive HIV-1-infected individuals compared to healthy controls. Our findings highlight a significant role for hnRNPA0 in HIV-1 replication and suggest that its IFN-I-regulated expression levels are critical for viral fitness allowing replication in an antiviral environment.

IMPORTANCE RNA-binding proteins, in particular, heterogeneous nuclear ribonucleoproteins (hnRNPs), have been extensively studied. Some act as host dependency factors for HIV-1 since they are involved in multiple cellular gene expression processes. Our study revealed hnRNPA0 as an IFN-regulated host factor, that is differently expressed after IFN-I treatment in HIV-1 target cells and lower expressed in therapy-naïve HIV-1-infected individuals. Our findings demonstrate the significant pleiotropic role of hnRNPA0 in viral replication: In high concentrations, hnRNPA0 limits viral replication by negatively regulating Tat-LTR transcription, retaining unspliced mRNA in the nucleus, and significantly impairing programmed ribosomal frameshifting. Low hnRNPA0 levels as observed in IFN-treated THP-1 cells, particularly facilitate HIV LTR activity and unspliced mRNA export, suggesting a role in innate immunity in favor of HIV replication. Understanding the mode of action between hnRNPA0 and HIV-1 gene expression might help to identify novel therapeutically strategies against HIV-1 and other viruses.

The human immunodeficiency virus type 1 (HIV-1) is the causative agent of the acquired immunodeficiency syndrome (AIDS). HIV-1 is highly adapted to the human host and can exploit various host factors (1–3) and hijack essential cellular processes for its replication. After infection of a susceptible host cell, predominantly CD4$^+$ T cells and macrophages, the single-stranded 9.7 kb long RNA is reverse-transcribed into double-stranded DNA, which then is irreversibly integrated into the genome of the host cell (4, 5). HIV-1 uses a variety of cellular mechanisms to express its complex genome: The HIV-1 replication strategy includes alternative splicing of its pre-mRNA (6) by a diverse network of splicing-regulatory-elements (SREs) acting in *cis*- and cellular RNA-binding proteins (RBPs) in *trans*-binding SREs (7). By binding the *cis*-regulatory elements, heterogeneous nuclear ribonucleoproteins (hnRNPs) and serine/arginine-rich-splicing factors (SRSFs) play a crucial role in alternative splicing and are thus essential for HIV-1 replication. To further expand the genetic repertoire, HIV-1 induces a programmed ribosomal frameshift (−1 PRF) to translate two of its three reading frames, resulting either in the synthesis of the viral structural proteins Gag (matrix, capsid, nucleocapsid) or upon −1PRF, additionally allows the generation of viral enzymes Gag-Pol (protease, reverse transcriptase, integrase) (8).

Most hnRNPs exhibit ubiquitous expression across cell types and tissues (9) (Human Protein Atlas proteinatlas.org). They selectively bind conserved RNA motifs, potentially exerting regulatory effects on the stability, subcellular localization, processing, and functionality of both cellular and viral RNAs (10). hnRNPA1, A2/B1 (11–17), and to a lesser extent hnRNPA3 (7, 18–21) have been extensively studied in many aspects and several studies focusing on HIV-1 gene expression are published for this protein family (22, 23). However, knowledge regarding hnRNPA0 in the context of viral infections remains notably limited.

At 305 aa in length, hnRNPA0 is the shortest member of the hnRNPA/B family and preferably binds to adenylate-uridylate (AU)-rich elements (AREs), which are commonly located at 3′-untranslated regions (UTRs) of mRNAs (24–27). The consensus motif of the AREs bound by hnRNPA0 is the pentamer AUUUA (26), which is notably also bound by hnRNPA1 (28). Through the sharing of binding sites, hnRNPs can synergistically collaborate and perform analogous functions or mutually compensate for each other (29–31). Nonetheless, occupancy of identical sequences does not inherently entail catalyzing identical processes (29). Moreover, despite the ability to bind similar target sequences, Drosophila homologs of the A/B family continued to demonstrate distinct functionalities (32).

By binding to the AREs of the respective mRNAs, hnRNPA0 is also involved in the processing of immunomodulatory mRNAs encoding tumor necrosis factor alpha (TNF-alpha), cyclooxygenase 2 (Cox-2), and macrophage inflammatory protein-2 (MIP-2) (26). Furthermore, mutation analysis revealed that hnRNPA0 is involved in the ERK/MAPK signaling pathways, which also play a crucial role in cell growth, cell differentiation, cell survival, cell migration, and cell division (33). So far, it remains unclear whether hnRNPA0 might also affect viral replication.

Since other members of the hnRNPA/B subfamily are described to modulate gene expression of cellular and viral genes, here, we investigated the impact of hnRNPA0 on HIV-1 replication, focusing specifically on post-integration steps.

RESULTS

The structural outlier of the hnRNPA/B family, hnRNPA0, acts as an interferon-repressed gene (IRepG)

Interferons play a critical role in limiting HIV-1 replication by inducing an antiviral state in the infected host and bystander cells (34, 35). Previously, we were able to show that IFNα14, the most potent IFN-I against HIV-1 (36, 37), strongly represses the expression of the RNA binding cellular host factor SRSF1 (38), thereby modulating HIV-1 gene expression, replication, and infectivity. This novel property of interferons, modulating the expression of cellular host factors, underscores that not only interferon-stimulated genes (ISGs) but also interferon-repressed genes (IRepGs) significantly determine the induced antiviral state within a cell (39). To investigate whether the expression of the second group of RNA-binding proteins with RNA-modulating effects, hnRNPs, is also influenced by interferons, we conducted a screening of several hnRNPs in IFNα14-treated, differentiated THP-1 cells (Fig. 1A). We noted significant downregulation exclusively of hnRNPA0 and hnRNPA1 mRNAs compared to the control, with hnRNPA0 exhibiting the most pronounced decrease. Both hnRNPs belong to the hnRNPA/B family which consists of four members that are hnRNPA0, A1, A2B1, and A3. However, in contrast to hnRNPA1, which has been particularly studied in the context of HIV-1 gene expression (7), little is known about the role of hnRNPA0. Point-accepted mutation analysis (Fig. S1) revealed that hnRNPA0 is quite distinct from the other hnRNPA/B members, despite carrying all main characteristics, two RNA-recognition-motifs (RRM), and an unstructured glycine-rich region (Fig. S1b) (40). In particular, the C-terminally located glycine-rich region of hnRNPA0 differs compared to the other family members (Fig. S2). HnRNPA0 exhibited the highest similarity to hnRNPA2B1 (score: 0.577), while hnRNPA1, A2B1, and A3 had an average PAM score of 0.264, revealing a higher degree of similarity.

To characterize the temporal IFN-mediated regulation of hnRNPA0, we treated THP-1 (Fig. 1B through E) and Jurkat cells (Fig. 1F through I) with IFNα14. We additionally included IFNα2 since it is used in the clinical treatment of chronic viral infections like the Hepatitis B virus (41). *ISG15* was used as a surrogate marker for IFN-stimulated genes (ISGs). The mRNA expression of *hnRNPA0* in THP-1 cells was significantly reduced after 8 h, while the strongest repression was observed at 12 h (2.8-fold; $P < 0.0001$) post-treatment. After 24 h, the mRNA expression increased until it was almost recovered after 48 h. A similar, although stronger and longer-lasting, effect was observed when THP-1 cells were treated with IFNα14. In Jurkat T cells, *ISG15* expression after IFNα2 treatment was strongly induced 4 h and 8 h post-stimulation, but the levels rapidly declined after 12 h (Fig. 1F). The *ISG15* expression in IFNα14-treated Jurkat cells was high and long lasting, and comparable to IFN treated THP-1 cells. While no alteration in *hnRNPA0* expression was observed in IFNα2-treated Jurkat cells, a trend for lower *hnRNPA0* mRNA levels 8–24 h post-treatment with IFNα14 was observed. Strikingly, a significant (1.8-fold; $P = 0.0233$) increase in mRNA levels was measured 48 h post-stimulation. As we observed the strongest reduction in *hnRNPA0* mRNA levels in IFNα14-treated THP-1 cells, we also confirmed the decrease in protein amount under these conditions using Western blot analysis (Fig. 1J and K).

Lastly, primary monocyte-derived macrophages (MDMs) from healthy donors were isolated and treated with IFNα14 (Fig. 1L and M). *ISG15* expression was strongly and persistently induced to levels comparable to stimulated THP-1 cells. Notably, following initial repression of *hnRNPA0* expression from 4 to 8 h in MDMs after IFNα14 treatment, *hnRNPA0* levels increased twofold by 24 h post-treatment compared to the PBS control.

These results further emphasized that hnRNPA0 is differentially regulated by IFN-I in a cell-type specific manner and acts as a transient IRepG.
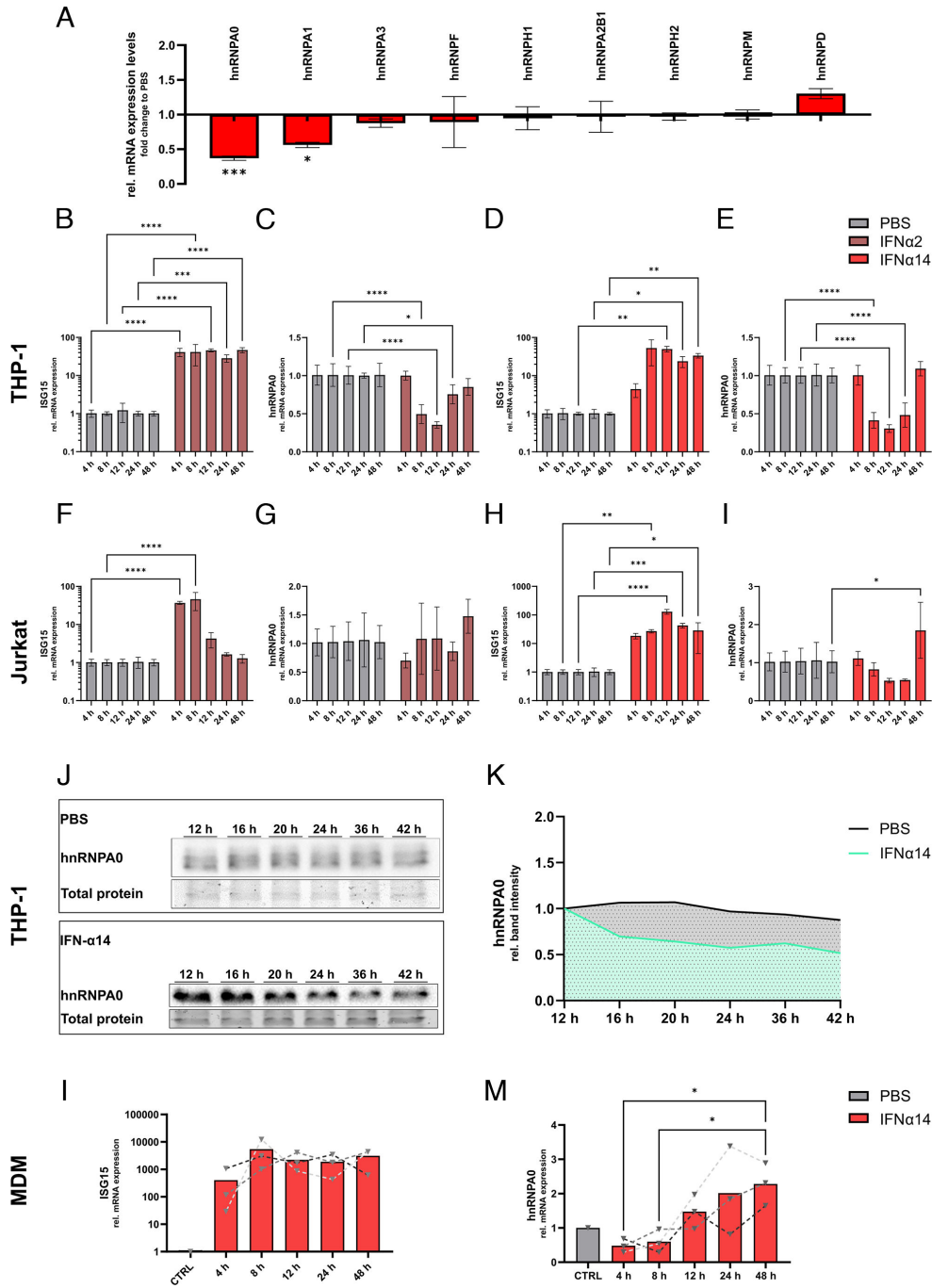
FIG 1 hnRNPA0 mRNA and protein levels are decreased upon IFN stimulation in HIV target cells. Differentiated THP-1 cells were treated with IFNα14 (500 UI/mL) or PBS. 8 h post-treatment cells were lysed, RNA was isolated and the expression levels of the respective hnRNPs was analyzed *via* RT-qPCR and normalized to *GAPDH* and *ACTB* expression levels. Differentiated THP-1 (B–E) or Jurkat (F–I) cells were treated with IFNα2 (dark red) or IFNα14 (bright red) (10 ng/mL). At the indicated time points, cells were lysed and subjected to the respective read-out. (B–I) mRNA expression of (B,D,F,H) ISG15 and (C,E,G,I) hnRNPA0 in THP-1 and Jurkat cells upon IFN treatment RT-qPCR was performed to monitor expression levels. *ACTB* was used as a loading control. (J,K) THP-1 cells were treated with 10 ng/mL IFNα14. Proteins were separated by SDS-PAGE, blotted on a nitrocellulose membrane, and analyzed using an antibody against hnRNPA0. Total protein amounts were stained using trichloroethanol and used for normalization. (J) Representative Western blots of hnRNPA0 from THP-1 cells treated with PBS or IFNα14. (K) The mean values of the quantification of four independent Western blots per condition are shown. (L,M) Monocyte-derived macrophages were treated with 10 ng/mL IFNα14. At the indicated time points, cells were lysed and

(Continued on next page)

FIG 1 (Continued)

RNA was isolated to evaluate mRNA expression levels *via* RT-qPCR of (L) ISG15 and (M) hnRNPA0. Expression levels of three independent experiments are shown. The mean values (+SD) of four biological replicates are shown in (A). (B–I) Mean (+SD) is shown for four independent experiments (B-E) at 12–48 h containing three replicates. (A) Two-way ANOVA, (B–I) two-way repeated-measures ANOVA with Šidák multiple comparisons test, and (L,M) one-way repeated-measures ANOVA with Dunnett post hoc test were performed to evaluate whether the differences between the groups reached statistical significance (*$P <$ 0.05, **$P <$ 0.01, ***$P <$ 0.001, ****$P <$ 0.0001).

The expression levels of hnRNPA0 in HIV-1-infected cells are modulated by type I interferons in a JAK1/2-dependent manner

To investigate whether hnRNPA0 might be regulated by exogenous IFNs in HIV-1-infected cells, PMA-differentiated THP-1 cells were infected with the CCR5-tropic HIV-1 NL4-3 AD8 strain (42). Cells were treated with IFNα14 16 h post-infection and the JAK1-2 inhibitor ruxolitinib (Fig. 2) was added to test for IFN specificity. At the indicated time points, total cellular RNA was isolated and expression levels were analyzed *via* RT-qPCR. A significant increase in *ISG15* and *IFITM1* mRNA expression, used to monitor IFN stimulation, was observed upon IFN treatment throughout all time points (Fig. 2A and B). Of note, even though the ruxolitinib-treated cells showed elevated *ISG15* and *IFITM1* mRNA expression, the expression levels remained below the samples lacking the JAK-1/2 inhibitor. In agreement with previous studies, the induction of ISG15 and IFITM1 despite inhibition of JAK-1/2 could be explained by combinatory effects of the IFN treatment and viral sensing *via* TLRs (43–45) and STING (46). While the *hnRNPA0* mRNA expression levels of the ruxolitinib-treated cells were unaffected, we observed a reduction in *hnRNPA0* mRNA expression in the solely IFN-treated cells, already at 4 h post-treatment. After 8 h (2.6-fold; $P <$ 0.0001), the mRNA expression exhibited a significant decrease and continued to decline until 12 h post-treatment (2.6-fold; $P =$ 0,0001), but returned to its original levels after 48 h. These results indicated that in the context of HIV-1 infection, IFN-mediated suppression of hnRNPA0 is dependent on JAK1-/2 signaling.

Low levels of hnRNPA0 facilitate HIV-1 Tat-mediated LTR activity and unspliced RNA trafficking

Given the IFN-mediated repression of hnRNPA0, a scenario potentially mirrored during infection, we tested whether reduced hnRNPA0 levels could impact HIV-1 replication. As hnRNPs are ubiquitously involved in RNA processing, we initially analyzed HIV-1 LTR activity in the presence of Tat and depleted levels of hnRNPA0 using siRNA. Using a reporter cell line harboring a stably integrated luciferase expression cassette under the control of the NL4-3 LTR promoter, hnRNPA0 knockdown resulted in a significant increase in LTR activity (1.9-fold $P =$ 0.0003) (Fig. 3A).

Since decreased viral replication might be caused by aberrant splice site usage, resulting in insufficient or unbalanced mRNA transcript amounts (7), RT-qPCR-driven analysis of HIV-1 splice site usage was conducted to investigate the potential influence of hnRNPA0 on HIV-1 alternative splice site usage. HIV-1 mRNA class-specific splicing patterns were analyzed using semi-quantitative RT-PCR (Fig. 3B) (38). We co-transfected cells with a plasmid encoding the proviral clone NL4-3 and siRNA against hnRNPA0. Despite a small increase in *vpr3* (4 kb-class), we did not observe any changes in the viral splicing pattern under depleted hnRNPA0 levels. Furthermore, we quantified the total viral mRNA (reflected by *exon 1* and *exon 7* expression). Confirming the previously observed increased transcriptional activity, we observed an increase in HIV-1 *exon 1* (1.8-fold; $P =$ 0.0187) and *exon 7* (1.5-fold; $P =$ 0.0124) containing mRNAs upon hnRNPA0 knockdown. In agreement with the semi-quantitative PCR approach, no significant changes in the viral splicing pattern were observed (Fig. 3C through F).

Since hnRNPA1 and A2B1 are known for nucleocytoplasmic shuttling, we investigated a potential post-mRNA-splicing influence of hnRNPA0 on mRNA trafficking. We transfected HEK293T cells with pNL4-3 and siRNA directed against hnRNPA0. 72 h
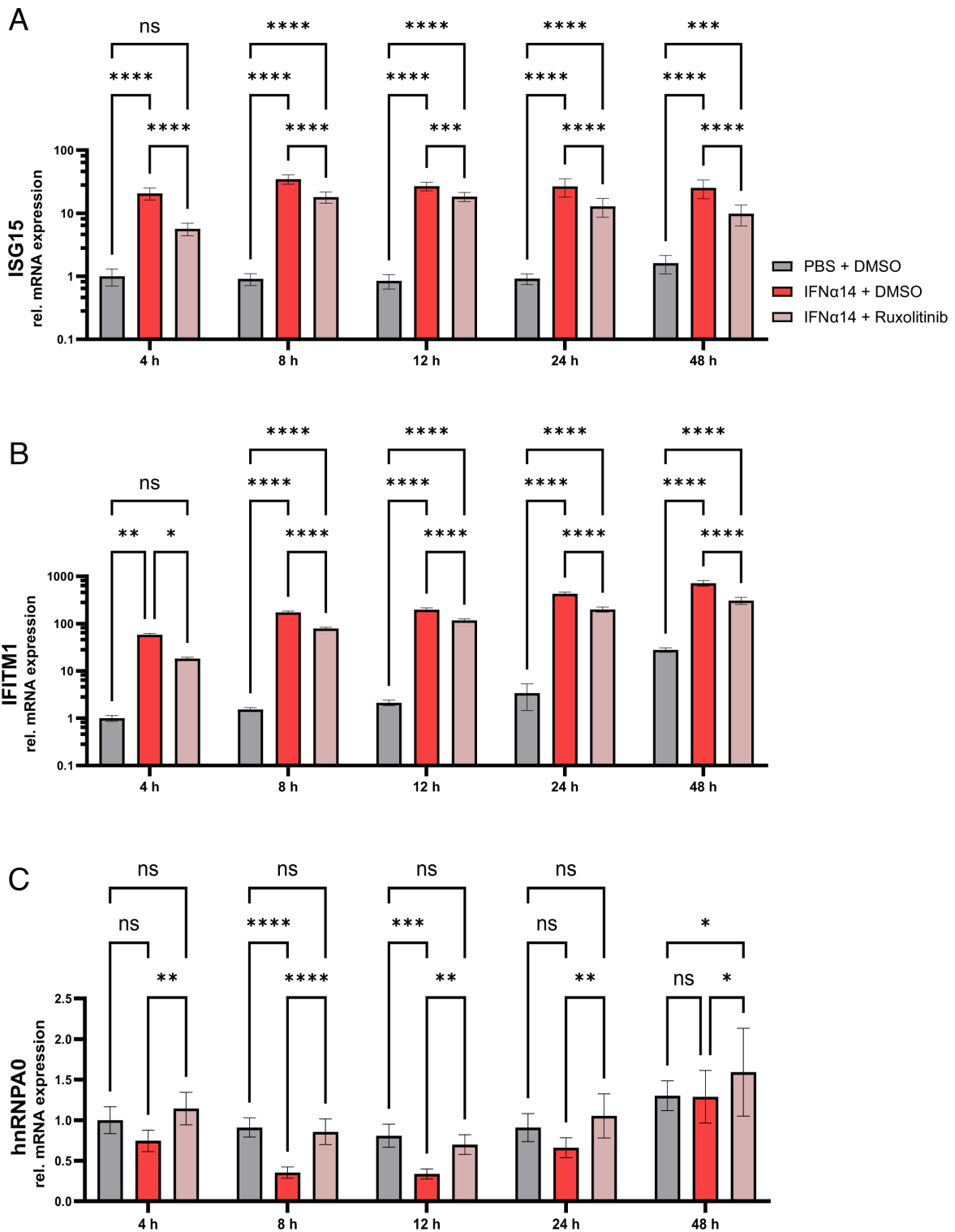
FIG 2 Interferon signaling regulates hnRNPA0 mRNA expression. Differentiated THP-1 macrophages were treated with 1 µM ruxolitinib or a DMSO solvent control 1 h before inoculation of the viral clone NL4-3 AD8 (MOI 1). 16 h post-infection cells were washed, and a medium containing 10 ng/mL IFNα14 or PBS and 1 µM ruxolitinib or DMSO was added. At the indicated time points post-treatment, cells were lysed and further subjected to RNA isolation. RT-qPCR was performed to monitor mRNA expression levels of (A) *ISG15* (B) IFITM1 and (C) hnRNPA0. Mean + SD is indicated. Statistical comparisons of the groups (two independent experiments each with four biological replicates) were performed using two-way ANOVA with Tukey's post hoc test. (*$P < 0.05$, **$P < 0.01$, ***$P < 0.001$, ****$P < 0.0001$ and ns, not significant).
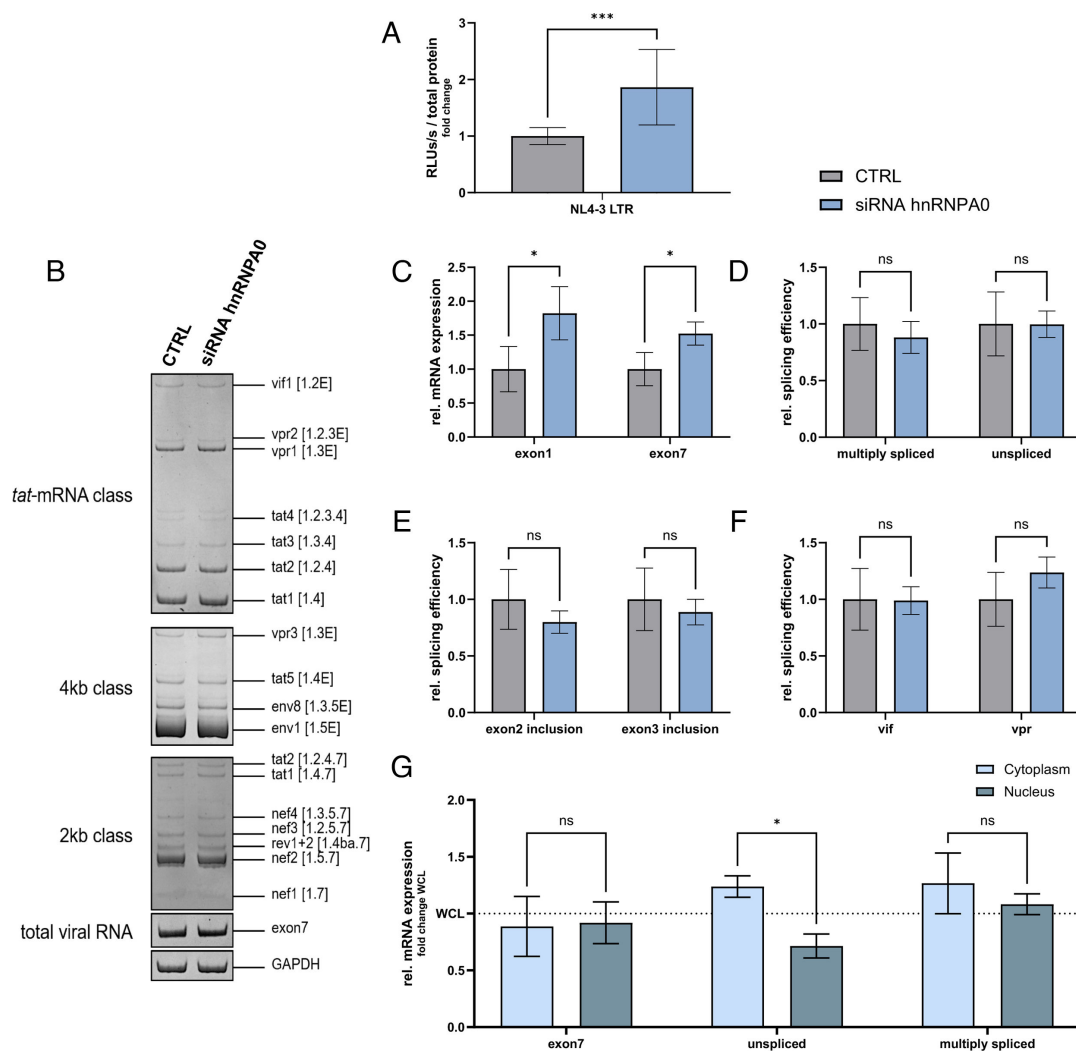
FIG 3 hnRNPA0 knockdown enhances HIV-1 LTR activity, does not affect its splicing pattern, and causes more efficient export of unspliced mRNA into the cytoplasm. (A) A549 LTR Luc-PEST reporter cells were transfected with a plasmid encoding the Tat protein (SVctat) as well as siRNA against hnRNPA0 or an off-target control. 48 h post-transfection cells were lysed and luciferase reporter assays were performed. The RLUs were normalized to the protein amount analyzed *via* Bradford assay. The reporter cell line was previously generated using the Sleeping Beauty system (47). The PEST sequence fused to the Firefly luciferase causes rapid degradation of the protein (48). (B–G) HEK293T cells were transfected with pNL4-3 as well as siRNA against hnRNPA0 or an off-target control. 72 h post-transfection cells were lysed, RNA isolated and RT-qPCR was performed to evaluate expression levels. (B) RT-PCR was performed using primer pairs covering viral mRNA isoforms of the 2 kb, 4 kb, and tat-mRNA-class (described in reference (38)). Primers covering HIV-1 exon 7 containing transcripts were used for normalization of whole-viral-mRNA and cellular GAPDH was included as loading control. The HIV-1 transcript isoforms are labeled according to reference (49). The amplified PCR products were separated on a 12% non-denaturing polyacrylamide gel. (C) Expression levels of exon 1 and exon 7 containing mRNAs (total viral mRNA) were normalized to GAPDH. (D–F) Expression levels of (D) multiply spliced and unspliced mRNAs, (E) exon 2 and exon 3 containing mRNAs, (F) *vif* and *vpr* were normalized to exon 1 and exon 7 containing mRNAs (total viral mRNA). (G) Prior lysis, cells were transferred into reaction tubes, and the cytoplasmic fraction was separated from the nuclei using a hypotonic buffer. The RNA of each fraction was isolated, and expression levels of HIV-1 exon7 containing, unspliced, and multiply spliced mRNAs were analyzed. *GAPDH* and *ACTB* were used as loading controls, with intron-specific primers used for the nuclear fraction. Fractionation was confirmed using several primers specific for nuclear or cytoplasmic abundant mRNAs. Expression levels were initially normalized to the control siRNA and further normalized to the values of another unfractionated control plate termed whole-cell lysates (WCL). The mean (+SD) of 12 independent replicates from two biologically independent experiments for (A), four biological replicates for (C–F), and six biological replicates of three independent biological replicates for (G), two independent biological replicates for the cytoplasmic fraction of unspliced mRNA. (A–F) Unpaired two-tailed *t*-tests were calculated to determine whether the difference between sample groups reached the level of statistical significance (*$P < 0.05$, **$P < 0.01$, ***$P < 0.001$, ****$P < 0.0001$ and ns, not significant) for (G) an ordinary two-way ANOVA was performed.

post-transfection, we lysed the cells, separated the nuclear and cytoplasmic fractions, and analyzed the HIV-1 transcript levels in comparison to whole-cell lysates (WCL). We detected significantly less unspliced mRNAs in the nucleus of cells with depleted hnRNPA0 levels (0.6-fold; $P = 0.0289$), whereas *exon 7* containing mRNAs and multiply spliced mRNAs did not show any significant changes between the nuclear and cytoplasmic fractions. Thus, hnRNPA0 knockdown enhances HIV-1 LTR activity, and unspliced mRNA export while not affecting HIV-1 splicing patterns.

Low hnRNPA0 levels facilitate HIV-1 particle production and viral replication

As low levels of hnRNPA0 promote HIV-1 Tat-LTR-mediated transcription and facilitate the nuclear export of unspliced HIV-1 mRNAs, we next tested whether the enhanced transcriptional activity under low hnRNPA0 conditions would result in a higher replication rate.

To analyze the impact of the combined effects on virus production and infectivity, we analyzed the viral supernatant of anti-hnRNPA0 siRNA-treated HEK293T cells. This siRNA knockdown procedure resulted in significant reduction in hnRNPA0 protein levels (4.5-fold; $P = 0.0011$) (Fig. S3a and b). As determined by p24-CA-ELISA, we observed significantly more viral particles (1.5-fold; $P = 0.0002$) (Fig. 4A) and HIV-1 genome copies (1.4-fold; $P = <0,0001$; Fig. 4B) in the supernatant. To determine whether low hnRNPA0 levels might facilitate viral replication even in the presence of host restriction factors, we transfected cells stably expressing APOBEC3G (A3G) with an anti-hnRNPA0 siRNA and an NL4-3 encoding plasmid. A3G levels were not affected by the treatment (Fig. S3). Low hnRNA0 conditions resulted in higher infectious viral particle production from cells with low and intermediate expression of A3G (Fig. 4C). At higher A3G levels, we did not observe a significant increase in infectious virus production. Thus, depleted hnRNPA0 levels facilitate HIV-1 infectivity even in the context of host restriction.

To confirm the findings above in the context of spreading infection, we next inoculated Jurkat T cells with HIV-1 NL4-3. hnRNPA0 levels were knocked down using anti-hnRNPA0 LNA GapmeRs, which are efficiently taken up by T cells *via* pinocytosis (50). 7 days post-infection, supernatants were harvested and subjected to p24-CA-ELISA and used to infect TZM-bl reporter cells. In agreement to previous results, a significant increase in particle production (1.7-fold; $P = 0.0133$, Fig. 4D) and infectivity (1.6-fold; $P = 0.0135$, Fig. 4E and F) was observed.

In conclusion, our data suggest that low hnRNPA0 levels facilitate viral replication and infectivity.

High levels of hnRNPA0 inhibit HIV-1 Tat-LTR activity, nuclear export of unspliced HIV-1 mRNA, and promote relative splicing efficiency of vif mRNA

As we also observed elevated hnRNPA0 expression levels in Jurkat and MDMs at late timepoints after IFN stimulation, we analyzed whether elevated levels of hnRNPA0 might negatively affect HIV-1 replication and directed our subsequent overexpression analyses toward luciferase-based LTR reporter assays. Cells were co-transfected with Tat-transactivated LTR-luciferase reporter constructs and a hnRNPA0 expression vector. In addition to the NL4-3 laboratory strain, we included 10 primary LTRs derived from HIV-1 transmitted-founder viruses (TFV, Fig. 5A). We observed an almost twofold reduction of the NL4-3 LTR ($P = 0.0028$) activity, while TFV LTR activities were repressed to an even higher degree. We also confirmed HIV-1 LTR inhibition in cells with an integrated LTR reporter confirming an inhibitory effect on plasmid-driven and integrated LTRs (Fig. S4g). Next, we investigated the impact of high hnRNPA0 levels on HIV-1 splice site usage and performed semi-quantitative RT-PCR (Fig. 5B) with mRNA-class-specific primers (38). High hnRNPA0 levels resulted in an increase *vif1*, *vpr2, tat2* (*tat*-mRNA-class), and *nef1* (2 kb-class) indicating an increase in exon 2 inclusion. *Vpr3, tat5* (4 kb-class), and *tat1* (2 kb-class) levels were slightly decreased. In agreement with the loss in LTR activity, RT-qPCR confirmed a strong reduction in total viral mRNA, measured by primer pairs targeting the initial and terminal HIV-1 exons 1 (2.9-fold; $P = 0.0089$) and 7 (4.6-fold; $P < 0.0001$). By using intron 1
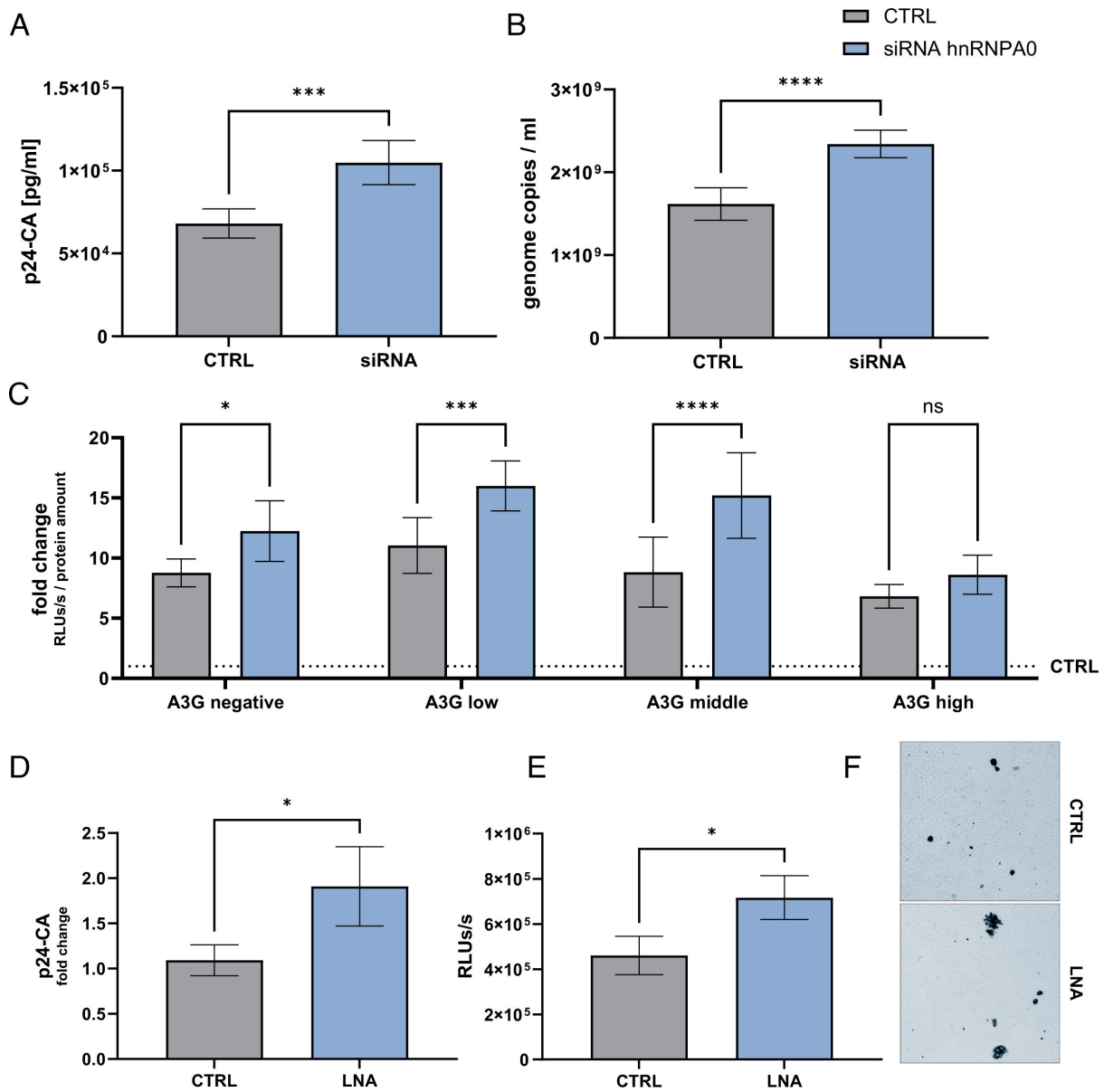
FIG 4 Knockdown of hnRNPA0 elevates viral particle production, copy numbers, and infectivity. (A–E) HEK293T cells were transfected with pNL4-3 as well as siRNA against hnRNPA0 or an off-target control. 72 h post-transfection (A,B), cells were lysed and Western blotting was performed to evaluate the protein amounts using the antibodies listed in Table 1. Supernatants were harvested and subjected to further analysis (C–E). (A) Representative Western blot of four independent replicates of the quantification (Mean + SD) shown in (B). For improved comparability, the samples were repositioned adjacently after imaging, as denoted by the dotted line. The depicted samples underwent processing on the same nitrocellulose membrane. Trichloroethanol was used for visualization of total protein amounts, which the signals were normalized to. Particle production was analyzed *via* (A) p24-Capsid-ELISA. (B) RNA of the viral supernatant was isolated and RT-qPCR was performed to evaluate viral copy numbers. (C) A viral supernatant was used to infect TZM-bl reporter cells. 48 h post-infection, TZM-bl cells were lysed and the luciferase activity was measured. The relative light units were normalized to the total protein amount analyzed *via* Bradford assay. Mean (+SD) is shown for four independent replicates of (C), six of (D), and four of (E) with two technical replicates each. (F–H) Jurkat cells were infected with NL4-3, using a MOI of 2. 24 h post-infection cells were washed and 12 µM of LNA GapmeRs directed against hnRNPA0 or a non-template control were added to the culture medium. 7 days post-infection, supernatants were harvested and particle production was analyzed *via* (F) p24-Capsid-ELISA. TZM-bl reporter cells were infected using the harvested supernatants and further analyzed *via* (G) luciferase assay and (H) X-Gal staining. Mean (+SD) is shown for (F,G) four biological replicates. Unpaired two-tailed *t*-tests were calculated to determine whether the difference between the sample groups reached the level of statistical significance (*$P < 0.05$, **$P < 0.01$, ***$P < 0.001$, ****$P < 0.0001$ and ns, not significant). For (C), the groups were compared by two-way ANOVA with Bonferroni post hoc test.

TABLE 1 Primary antibodies used in this study

Target	Supplier
hnRNPA0	Abcam (ab197023)
FLAG-tag	Abcam (ab49763)
HIV-1 Vif	Abcam (ab66643)
HIV-1 p24	Aalto (D7320)
APOBEC3G	HIV Reagent Program (ARP-10082)
HIV-1 p15	Abcam (ab66951)
HIV-1 Vpr	Proteintech (51143-1-AP)
Human CD11b	Biolegend (301306)
HIV-1 p24 ELISA pair	SinoBiological (SEK11695)
HIV-1 reverse transcriptase	Abcam (ab63911)

spanning primers and those covering the 2 kb class-specific exon junction D4-A7, we observed a trend toward more unspliced and significantly less multiply spliced mRNAs (0.8-fold; $P = 0.03$) (Fig. 5D). *Exon 2* containing transcripts were indeed detected more frequently ($P = 0.0088$), while those harboring *exon 3* were significantly less detected ($P = 0.0388$). When using a D1-A1-specific junction primer also detecting the *vif-mRNA-specific* intron, we observed a 1.8-fold ($P = 0.0424$) increase in the mRNA coding for the essential accessory protein Vif, which counteracts the host restriction factor APOBEC3G (51) and the cytosolic DNA sensor STING (52). Further usage of primers specific for the HIV-1 D1-A2 splice site junction and the *vpr* intron revealed a slight increase in the splicing efficiency of *vpr-mRNA*, coding for the pleiotropic accessory protein Vpr necessary for replication in myeloid cell types as dendritic cells (53).

Next, we analyzed the effect of high hnRNPA0 levels on RNA trafficking and co-transfected HEK293T cells with pNL4-3 and a hnRNPA0 encoding plasmid and subjected nuclear and cytoplasmic RNA to RT-qPCR analysis. Consistent with prior findings demonstrating reduced hnRNPA0 levels, our investigation revealed a notable increase in unspliced mRNA abundance within the nuclear fraction compared to the cytoplasmic fraction. Notably, there was no significant alteration observed in *exon 7*-containing or multiply spliced mRNA species. Altogether, these data reveal that high hnRNPA0 level impedes HIV-1 Tat-LTR activity, facilitates exon 2 inclusion and *vif* mRNA formation, and promotes the retention of unspliced HIV-1 mRNA within the nucleus.

High hnRNPA0 level limits HIV-1 particle production and viral replication

We next determined whether the inhibition of transcriptional and post-transcriptional steps under high hnRNPA0 conditions would alter HIV protein levels. Western blot analysis revealed that a 10-fold increase ($P = 0.0003$) in hnRNPA0 protein levels was accompanied by strong repression in p24 levels (3.0-fold; $P = 0.0009$) (Fig. 6A and B). Vif (1.9-fold; $P = 0.0319$) and Vpr (2.2-fold; $P = 0.023$) protein levels were also reduced, consistent with the splicing-efficiency observations described above. Furthermore, we revealed a dose-dependent shift between HIV-1 p15 and p55 at high hnRNPA0 conditions. Since both proteins are translated from an unspliced polycistronic mRNA, the shift in the p55/p15 ratio and p24/p15 ratio, respectively, implies an impact on viral frameshift efficiency (Fig. 6C). To strengthen our findings, we assessed the levels of p51 (RT), which demonstrated a similar decrease comparable to that of p15, indicative of their dependence on −1PRF. Finally, we confirmed the inhibition of ribosomal frameshifting using a dual luciferase reporter system encoding a constitutively accessible Renilla luciferase and a Firefly luciferase accessed *via* −1PRF-mediated recoding, both under the control of the CMV promoter (Fig. 6D). Of note, the CMV promoter activity of the transfected pcDNA3.1 plasmid was not affected by high hnRNPA0 levels, indicating a promoter specificity, but we observed inhibitory effects of hnRNPA0 overexpression in SV-40 driven plasmids (Fig. S4). Supporting the previous results, we observed a dose-dependent reduction of −1PRF efficiency upon increased hnRNPA0 levels (up to 5.5-fold; $P < 0.0001$). In accordance with this finding, we observed a significantly increased −1PRF activity in cells treated with
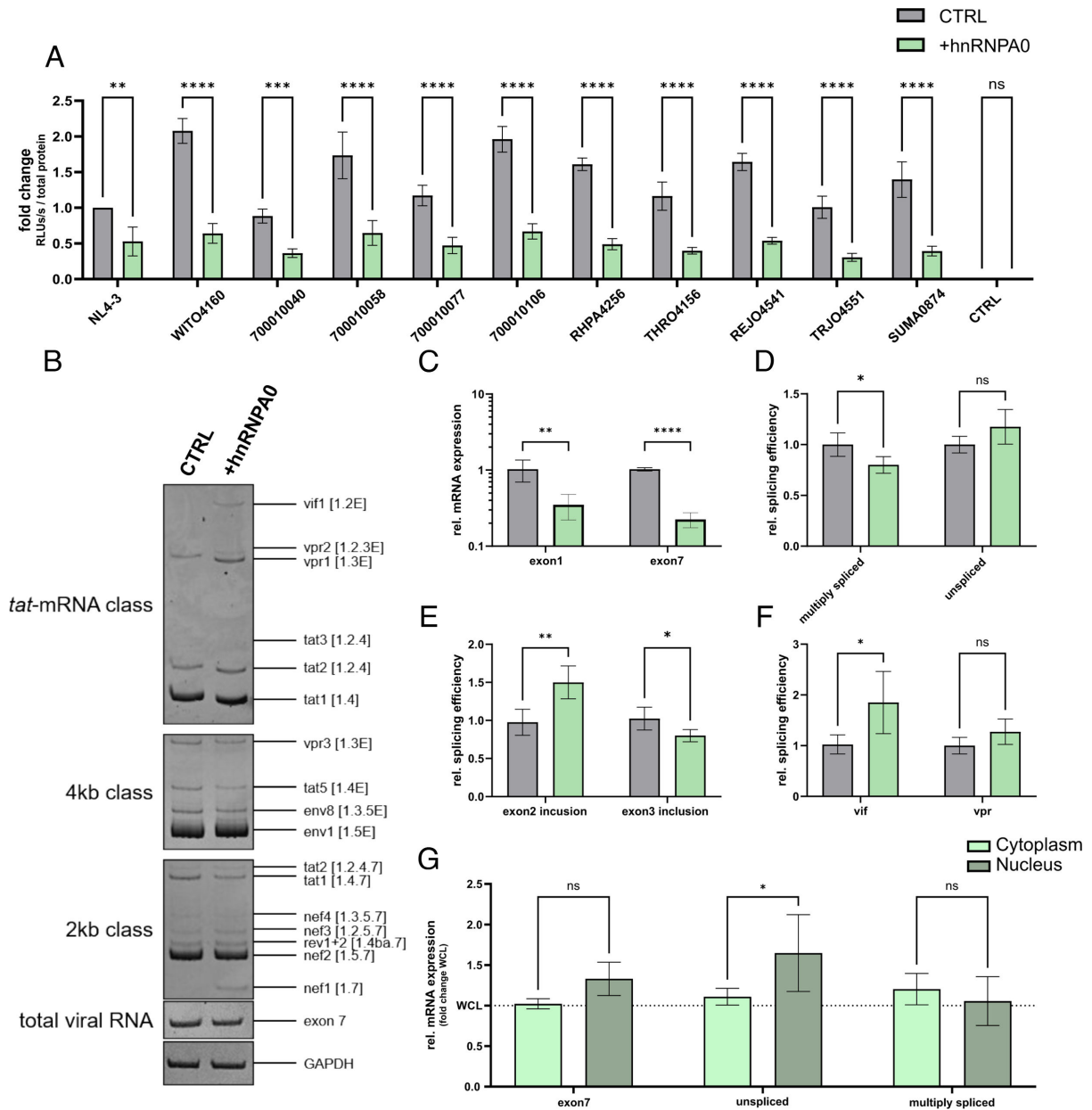
FIG 5 hnRNPA0 overexpression inhibits HIV-1 LTR activity, modulates its splicing pattern, and retains more unspliced mRNA in the nucleus. (A) Vero cells were transfected with plasmids coding for hnRNPA0 (pcDNA-FLAG-NLS-hnRNPA0), Tat (SVcTat), and Firefly luciferase reporter plasmids with LTR sequences from the proviral clone NL4-3 and sequences obtained from transmitted founder viruses from patient samples (54, 55) provided by Dr. John C. Kappes. A vector (pTA Luc) expressing only the Firefly luciferase was used as a control. 24 h post-transfection, the cells were lysed, and luciferase-based reporter assays were performed. The relative light units (RLUs) were normalized to the protein amount analyzed *via* Bradford assay. (B-G) HEK293T cells were transfected with a plasmid coding for the proviral clone NL4-3 (pNL4-3) and an expression vector encoding hnRNPA0 or empty vector control (pcDNA3.1(+)). 48 h post-transfection, RNA was isolated and subjected to further analysis. (B) RT-PCR was performed using primer pairs covering viral mRNA isoforms of the 2 kb, 4 kb, and tat-mRNA classes (described in reference (38)). Primers covering HIV-1 exon 7 containing transcripts were used for normalization of whole-viral-mRNA and cellular GAPDH was included as loading control. The HIV-1 transcript isoforms are labeled according to reference (49). The amplified PCR products were separated on a 12% non-denaturing polyacrylamide gel. (C) Expression levels of exon 1 and exon 7 containing mRNAs (total viral mRNA) were normalized to GAPDH. (D-F) Expression levels of (D) multiply spliced and unspliced mRNAs, (E) exon 2 and exon 3 containing mRNAs, (F) *vif* and *vpr* were normalized to exon 1 and exon 7 containing mRNAs (total viral mRNA). (G) Prior lysis, cells were transferred into reaction tubes, and the cytoplasmic fraction was separated from the nuclei using a hypotonic buffer. The RNA of each fraction was isolated and expression levels of HIV-1 exon7 containing, unspliced, and multiply spliced mRNAs were analyzed. *GAPDH* and *ACTB* were used as loading controls, with intron-specific primers used for the nuclear fraction. Fractionation was confirmed using several primers specific for nuclear or cytoplasmic abundant mRNAs. Expression levels were initially normalized to the control siRNA and further normalized to the values of another unfractionated (Continued on next page)

FIG 5 (Continued)

control plate termed whole-cell lysates (WCL). Mean (+SD) is shown for three biological independent replicates for (A), four biological replicates for (C–F), and six biological replicates of three independent biological replicates for (G). (A) two-way ANOVA with Dunnett post hoc test and (C–F) unpaired two-tailed t-tests were calculated to determine whether the difference between sample groups reached the level of statistical significance (*$P < 0.05$, **$P < 0.01$, ***$P < 0.001$, ****$P < 0.0001$ and ns, not significant) for (G) an ordinary two-way ANOVA was performed.

siRNA, resulting in lower expression of hnRNPA0 (Fig. S3c through e). Specifically, the p15/p55 ratio was shifted in favor of p15, which was confirmed using a dual luciferase frame shift reporter assay. Thus, hnRNPA0 is not only capable of modulating the HIV-1 LTR activity and mRNA export of unspliced mRNA, but it is also able to modify frameshifting efficiency. Altogether, these hnRNPA0-affected processes could impact viral replication.

Subsequent analysis of supernatants of pNL4-3-transfected HEK293T cells revealed a significant decrease in p24-CA production (threefold; $P < 0.0001$), viral copy numbers (>5-fold; $P = 0.0008$) in the supernatant, and production of infectious particles (twofold; $P < 0.0001$) under elevated hnRNPA0 levels (Fig. 6E through G).

We validated the above results by infecting a Jurkat cell line stably expressing a doxycycline-inducible hnRNPA0 cassette (4.7-fold; $P = 0.0039$; Fig. S5d). To ensure consistency with the previous assays, at 40 h post-infection, we prevented re-infections through AMD3100 treatment. We observed significantly less viral copies (0.8-fold; $P = 0,0318$) and a reduced amount of infectious virus in the supernatant (0.5-fold; $P < 0,0001$) (Fig. 6H and I), confirming that high hnRNPA0 levels inhibit viral replication, likely by interfering with plasmid-driven and integrated Tat-LTR activity, mRNA export, and −1PRF.

hnRNPA0 transcript levels are lower in HIV-1-infected individuals compared to healthy controls

To evaluate whether hnRNPA0 levels might be differently expressed in persons with HIV-1 (PWH) and whether the hnRNPA0 levels might depend on the infection and inflammation status, we analyzed PBMC samples from 10 donors without HIV-1, 8 acute and 11 chronic PWH, and 13 PWH under ART-treatment (Fig. 7). Elevated *ISG15* levels were observed in acute and chronic PWH, albeit the differences to controls were only significant for chronic PWH ($P = 0.0246$). Remarkably, acute ($P = 0.0483$) and chronic ($P = 0.0549$) PWH had lower *hnRNPA0* mRNA levels. For ART-treated PWH, we observed expression levels for both *ISG15* and *hnRNPA0* that were comparable to the control cohort.

Since in PWH, gastrointestinal lymphoid tissue (GALT) shows a more pronounced depletion of T cells (56, 57) than peripheral mononuclear blood cells (PBMCs), we additionally performed a comprehensive re-analysis of RNA sequencing data obtained from colonic lamina propria mononuclear cells LPMCs derived from PWH (Fig. S6). We observed concurrent upregulation of ISGs, including HIV-1 host restriction factors (58) and a significantly lower amounts of certain hnRNPs including A1, F, or K. In general, hnRNPA0 was relatively weakly expressed in GALT, but we observed that hnRNPA0 was 1.28-fold lower expressed in PWH, compared to controls (Fig. S6).

In conclusion, PWH had lower hnRNPA0 levels and concomitantly higher ISG15 levels, suggesting a physiologically relevant role for hnRNPA0 in the context of innate immunity against HIV-1.

DISCUSSION

Interferons (IFNs) play a crucial and indispensable role in the host's defense against viral infections. They are essential components of the innate immune response, being rapidly induced upon viral recognition (34, 35). IFNs activate a complex signaling cascade leading to the reprogramming of the cellular expression profile, by inducing interferon-stimulated-genes (ISGs) (59–61) and repressing interferon-repressed-genes (IRepGs), which collectively establish an antiviral state inhibiting viral replication, limiting viral spread, and enhancing overall antiviral immunity (62, 63).
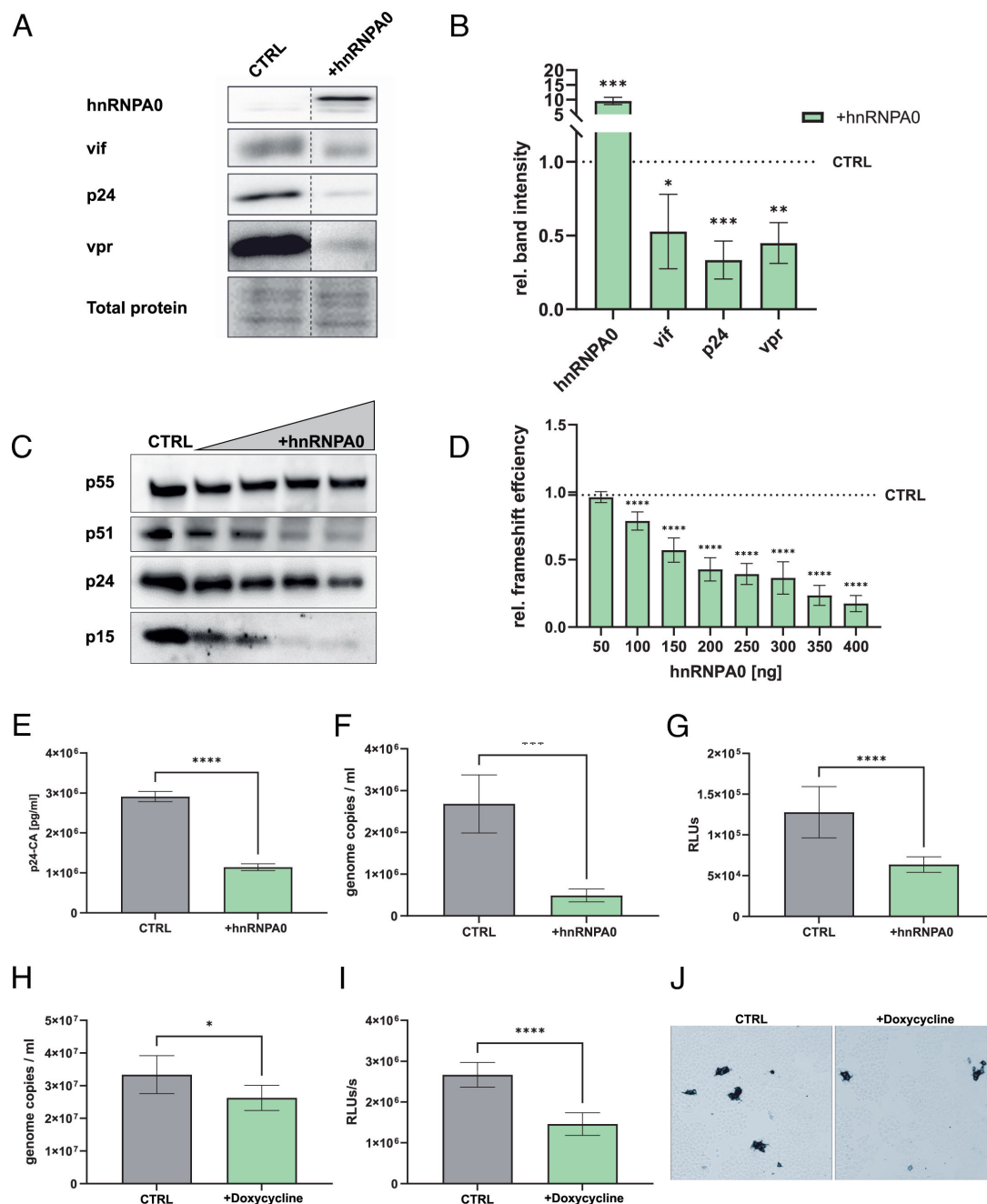
FIG 6 hnRNP A0 overexpression decreases HIV-1 protein levels, −1 PRF efficiency, particle production, and infectivity. HEK293T cells were transfected with a plasmid encoding the proviral clone NL4-3 and an expression vector coding for hnRNPA0. 48 h post-transfection, cells were lysed and the protein amounts were analyzed *via* Western blotting using the antibodies listed in Table 1. Trichloroethanol was used to stain total protein amounts, which were further used for normalization. (A) Representative Western blot of four independent replicates for the overexpression of hnRNPA0 quantified in (B). For improved comparability, the samples were repositioned adjacently after imaging, as denoted by the dotted line. The depicted samples underwent processing on the same nitrocellulose membrane. (C) HEK293T cells were transfected with pNL4-3 and increasing amounts of a plasmid encoding hnRNPA0 (250, 500, 1,000, and 1,500 ng). 48 h post-transfection, cells were lysed, proteins were separated *via* PAGE, and analyzed *via* immunoblotting using antibodies targeting p15 (also showing p55), p51, and p24. One representative Western blot of three independent experiments is shown (D) HEK293T cells were transfected with the indicated amounts of a plasmid encoding hnRNPA0. 6 h post-transfection, a second transfection was performed using luciferase reporter plasmids including the HIV-1 frameshift site. 24 h post-second transfection, the cells were harvested, and the Firefly to Renilla luciferase activity ratio was measured *via* luciferase reporter assay. In the luciferase reporter, the Renilla luciferase is positioned in-frame, facilitating translation during ribosomal scanning of the RNA, while the Firefly luciferase is placed in the −1-frame, yielding a functional polyprotein only upon occurrence of the −1 frameshift. The mean (+SD) of three biologically independent

(Continued on next page)

FIG 6 (Continued)

experiments with three replicates each is shown. For 350 and 400 ng, one experiment with three independent replicates was performed. (H–J) Using the Sleeping Beauty system, Jurkat cells were previously stably transfected with doxycycline-inducible hnRNPA0 expression cassettes. Cells were simultaneously inoculated with NL4-3 and treated with 1 µg/mL doxycycline. 40 h post-infection, cells were washed and treated with 250 nM AMD3100, and 1 µg/mL doxycycline. 72 h post-infection, viral supernatants were harvested. Viral genome copies were analyzed *via* RT-qPCR targeting Exon7 (H) and TZM-bl reporter cells were infected for (I) luciferase assay and (J) X-Gal staining. The mean (+SD) of six biological replicates is shown. Unpaired two-tailed *t*-tests were calculated to determine whether the difference between the sample groups reached the level of statistical significance ($*P < 0.05$, $**P < 0.01$, $***P < 0.001$, $****P < 0.0001$ and ns, not significant), for (D) mixed-effects analyses followed by Dunnett post hoc test were performed.

HIV-1 depends on the host cellular machinery to fully utilize its genome, encompassing processes such as transcription, pre-mRNA splicing, mRNA export, and translation. RBPs as members of the heterogeneous nuclear ribonucleoproteins (hnRNP) and serine-arginine-rich splicing factor (SRSF) families play indispensable roles in HIV-1 replication. Various RBPs from these families have been characterized for their interactions with HIV-1 and their functions as host dependency factors (HDFs).

Previously, we were able to show that the expression of SRSF1, an essential RBP and HDF, is modulated by IFN-I (38). In this study, we identified hnRNPA0 as an interferon-regulated gene, which is directly or indirectly regulated by a JAK1/2-dependent pathway. In fact, JAK1 can phosphorylate STAT1 (64) and STAT1 is defined as a transcription factor of hnRNPA0 by the *ENCODE Transcription Factor Targets* data set (65, 66). Which mechanism might facilitate repression in mRNA levels of hnRNPA0 remains unclear; however, it is plausible that STAT1 promotes the substantial transcription of hnRNPA0 mRNA, which subsequently underlies auto-regulation similar to what has been previously reported for various other hnRNPs (67–71). With hnRNPA0 preferably binding to AU-rich elements (AREs), which are predominantly located in the 3′ UTR, it is most likely that hnRNPA0 binds a regulatory element within its 3′ UTR and either inhibits or causes premature polyadenylation of its mRNA (72). Another regulatory level involves IFN-induced phosphorylation since hnRNPA0 can be phosphorylated by MAPK-activated protein kinases (MAPKAPKs) 2 and 3 (73). Particularly, MAPKAPK2 has been demonstrated to phosphorylate hnRNPA0 at Serine 84 residue in response to lipopolysaccharide (LPS) stimulation. In addition, hnRNPA0 is regulated by short RNAs complementary to ribosomal 5.8S RNA (74) and miR205HG which has been identified as a translational inhibitor (75). Nevertheless, further investigations are needed to elucidate the mechanisms underlying hnRNPA0 regulation upon IFN treatment.

Mechanistically, RBPs were described to positively or negatively influence the transcriptional efficiency of HIV-1 by interacting with the viral LTR promoter region affecting the recruitment of transcriptional regulators (76–78), thereby influencing the overall production of viral RNAs (38). During HIV-1 replication, multiple spliced and unspliced mRNA transcripts are produced and regulated by alternative splice site usage, a process decisively regulated by SRSFs and hnRNPs.

Increased concentrations of hnRNPA0 *in vitro* resulted in a pronounced reduction in both viral particle production as determined by p24-ELISA and RT-qPCR, and diminished numbers of infected TZM-bl reporter cells (Fig. 6), reflecting its antiviral efficacy. Nevertheless, the cause behind this phenomenon did not stem from inefficient utilization of alternative splice sites, a factor extensively investigated in various HIV gene expression studies within the context of hnRNP-mediated regulation (42, 79–82), but rather due to a decrease in Tat-LTR activity and loss of total viral mRNAs (Fig. 6B). Although *in silico* mapping of hnRNPA0 to the NL4-3 genome revealed a strong binding affinity toward D4 (3.97 Z-score) (Fig. S7; Table S3), we did not observe a major effect on alternative spice site usage under high hnRNPA0 conditions. Despite not obtaining the highest Z-scores (max. 3.18), several hnRNPA0-binding sites are also located within the HIV-1 LTR (Fig. S8) suggesting a role in promoter regulation. Certain hnRNPs might interact with other nucleic-acid-binding proteins either *via* their auxiliary domain, which in the case of hnRNPA1 is the unstructured glycine-rich domain (83, 84) or *via* the RBD in the case of hnRNPA2B1 (13). Therefore, hnRNPA0 could act as
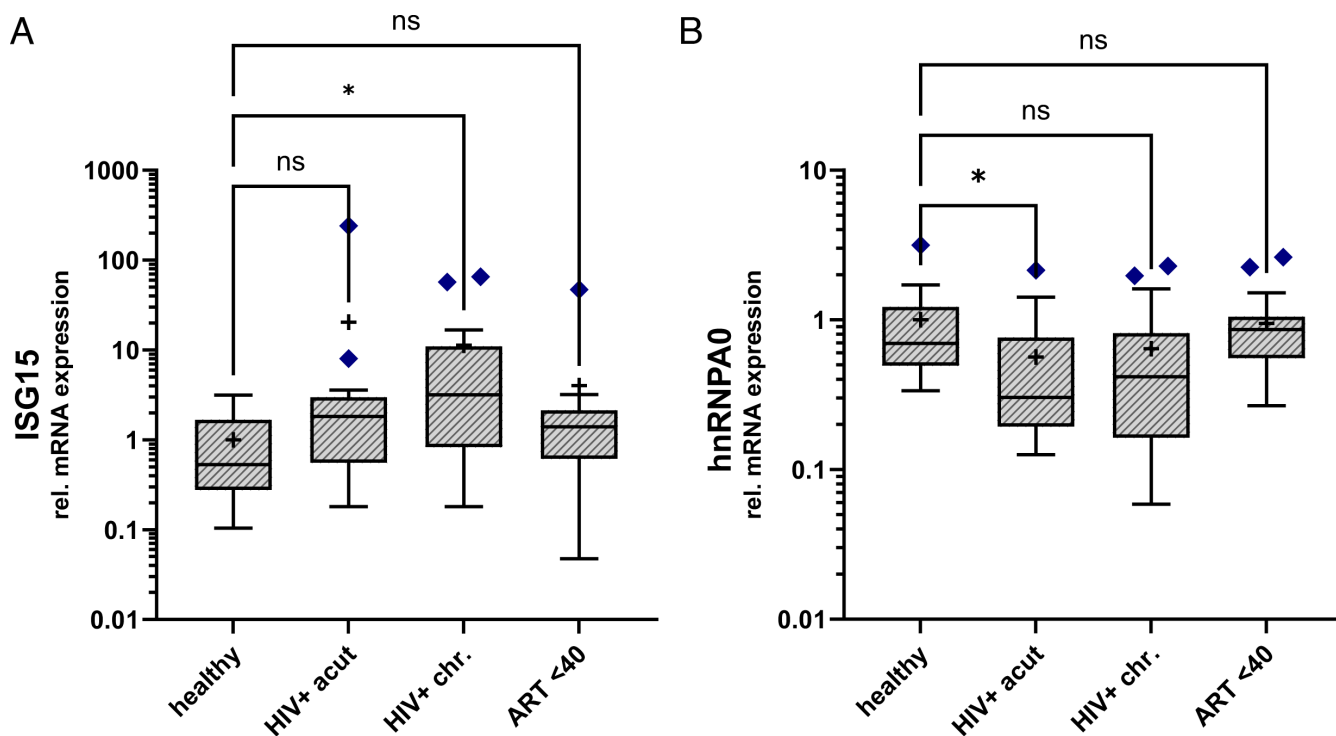
FIG 7 ISG15 and hnRNPA0 mRNA expression levels in HIV-1-infected cohorts. Relative expression levels of (A) ISG15 and (B) hnRNPA0 of PBMCs of healthy, HIV acutely infected, HIV chronically infected, and HIV-infected ART-treated individuals. ART <40 patients were below 40 copies/mL (measured by RT-qPCR). ACTB was used for normalization. The mean is indicated as "+." Error bars are indicated as Tukey min and max values. Purple rectangles represent outliers that were not included in statistical analysis. PMBCs were isolated from 11 healthy donors, 13 with acute HIV-1 infection, 17 treatment-naïve patients with chronic HIV-1 infection, and 17 HIV-1-infected patients on ART. Kruskal-Wallis test with Dunn's post hoc multiple comparisons test was used to determine whether the difference between the sample groups reached the level of statistical significance (*$P < 0.05$, and ns, not significant).

mediator facilitating LTR transcription by binding or scaffolding of other nucleic-acid-related proteins, already observed for other hnRNPs (85–89). In addition, hnRNPA0 could potentially interact with the 7SK particle, which binds and thus inhibits the function of P-TEFb (90) crucial for HIV-1 transcriptional elongation (91). Notably, the knockdown of hnRNPA1 and A2B1 (92, 93) attenuated the dissociation of P-TEFb from the 7SK complex, resulting in more active P-TEFb. However, based on our results, hnRNPA0 would rather facilitate the inhibition, that is binding of P-TEFb by the 7SK complex. Although we cannot exclude the mentioned possibilities, it seems more reasonable that hnRNPA0 might directly bind to the LTR as we observed a decrease in LTR activity under depleted hnRNPA0 levels in the absence of Tat (Fig. S9). By using electrophoresis mobility shift assays (EMSA), DNA-binding capacity has been observed for several hnRNPs, including hnRNPA1 (94) and A3 (95), the latter one binding DNA via its RNA-recognition-motif 1 (RRM1) domain. Furthermore, hnRNPK (96–101) and U were not only able to bind DNA but were also directly involved in transcription (102), with hnRNPK primarily known as a transcription factor. Moreover, it has been reported that hnRNPA1 and A2B1 can exert opposing effects on HIV-1 particle production and infectivity, with repression under high expression levels and enhancement under low expression levels. The observed effects were predominantly attributed to their impact on viral transcriptional activity. Importantly, hnRNPA3 showed no significant effect on viral replication, highlighting the selective role of hnRNPA/B family members in HIV-1 gene regulation (76). Furthermore, a competitive binding interaction, which resulted in the repression of the LTR activity when Tat was present, was already observed for the RBP SRSF1 by binding to overlapping sequences within TAR and the 7SK RNA (77). Notably, SRSF1 also increased the basal level of viral transcription when Tat was absent, a comparable observation was made for

hnRNPA0 in our study (Fig. S9). The hypothesis that hnRNPA0 competitively binds to the LTR is further supported by the increased LTR activity of the siRNA-transfected reporter cells (Fig. 3A). However, further studies are needed to elucidate the mode of action.

The involvement of hnRNPA0 in RNA trafficking so far has not been observed. Other hnRNP family members as hnRNPA1 (103, 104) and A2B1 (13, 105), however, are known to transfer mRNA from the nucleus into the cytoplasm facilitated by the C-terminally located M9 transport signal which facilitates nucleocytoplasmic shuttling through interactions with transportin-1 (106). Using immunofluorescence and mutational analysis, Yamada et. al identified two motifs within the M9 sequence essential for shuttling of hnRNPA1. The authors postulated that the N-terminal "SNFGPMK" and the C-terminal "PY" motifs are indispensable for the nucleocytoplasmic shuttling of hnRNPA1. Nevertheless, structural investigations have revealed that while the N-terminal sequence can exhibit greater diversity, the presence of the C-terminal "PY" motif, with one arginine in close proximity in the N-terminal direction, remains crucial. Furthermore, hnRNPA2B1 with the N-terminal sequence "SNYGPMK" is also able to shuttle between nucleus and cytoplasm. Both motifs are also present in hnRNPA0 with the N-terminal motif being "SSYGPMK," and one arginine located 5 instead of 4 AA upstream of the "PY" motif (107). In addition, hnRNPA0 has been identified both as a nuclear and cytoplasmic RBP in neurons (108) confirming its shuttling capacity. However, it is worth noting that, given that we observed significant changes solely for the unspliced mRNA, it is also possible that hnRNPA0 is not directly involved in mRNA trafficking but rather influences the protein levels of Rev, which is responsible for the export of unspliced HIV-1 mRNA (109).

During PRF, the ribosome shifts the viral reading frame (−1) at a specific RNA secondary site in the Gag-Pol overlap region during translation, allowing the production of the Gag-Pol polyprotein (110). HIV-1 uses −1PRF to maintain the correct stoichiometry of Gag and Pol proteins, which are essential for virion assembly and maturation (111). In this study, we demonstrated that hnRNPA0 significantly regulates HIV-1 frameshifting, although we cannot discriminate between a direct or indirect role. Previously described proteins that regulate viral −1PRF include the zinc finger antiviral protein (ZAP) (112) and the interferon-stimulated gene C19Orf66 (Shiftless, SFL) (113). Of note, in the SARS-CoV-2 context, hnRNPH1 and H2 were shown to reduce −1PRF in an intensity comparable to ZAP (112). Studies have demonstrated that the binding affinity between SFL and its target RNA can be influenced by RBPs (114). It is therefore intriguing to hypothesize that hnRNPA0 may act as a chaperone for SFL, facilitating its association with HIV-1 mRNA and thereby promoting frameshift inhibition.

Treating HIV-1 target cells with IFNα2 and IFNα14 revealed cell-type and IFN-specific differences with macrophages showing the strongest effects. Interestingly, THP-1 cells and MDMs differed in their expression patterns as overexpression of hnRNPA0 was observed in primary cells but not in the THP-1 model, even when we additionally monitored later time points (data not shown).

Simultaneous with elevated *ISG15* mRNA expression, we detected diminished levels of *hnRNPA0* mRNA in PBMCs derived from both acutely and chronically HIV-1-infected individuals. Nevertheless, the consequences of interferon-induced downregulation of hnRNPA0, albeit transiently, remain ambiguous within the *in vivo* setting.

However, it is conceivable that the interferon-mediated downregulation of hnRNPA0 contributes to the establishment of a favorable environment for the virus to replicate despite the presence of host restriction factors. Our findings, however, suggest that individual dependency factors such as hnRNPA0 or, as previously described SRSF1, exert only a modest effect alone (38). Nonetheless, the cumulative impact of numerous minor effects collectively determines replication efficiency.

Depleted hnRNPA0 levels significantly increased the LTR activity and consequently resulted in higher production of infectious viral particles (Fig. 4). In addition, low hnRNPA0 level facilitated −1PRF and the nuclear export of unspliced mRNAs (Fig. S3). At present, it remains uncertain whether this phenomenon contributes to facilitating

viral replication during acute infection and necessitates further investigation. Consistent with prior studies (115), the expression levels of hnRNPA0 in ART-treated patients were found to be comparable to those in the naïve cohort. This observation suggests that only ongoing viral replication may result in decreased hnRNPA0 levels due to heightened Jak1/2 induction (116), thereby partially compensating for the direct antiviral effects exerted by ISGs and restriction factors by higher LTR activity.

This study has limitations as the full role of hnRNPA0 remains unclear due to its pleiotropic functions. We identified hnRNPA0 as an RNA-binding protein regulated by IFN-I, affecting HIV-1 replication. However, mutational analysis to identify hnRNPA0 responsive binding sites in the LTR sequence and mechanistic insights into the inhibitory effect on ribosomal frameshifting are pending. However, since 576 UA-rich potential binding sites for hnRNPA0 with 17 exclusively within the LTR region are predicted in the NL4-3 genome (Table S3), an arduous genome-wide analysis of *cis*-regulatory elements is needed to further elucidate HIV-1 regulation by hnRNPA0. Subsequent studies are needed to confirm protein binding attenuation through RNA-pulldown experiments.

HnRNPs might interact with the viral RNA genome and facilitate its packaging into new viral particles during the assembly process. Furthermore, hnRNPs might impact the stability of HIV-1 RNA by binding to specific regions within the viral transcript and influencing its degradation or stabilization. No packaging and stability studies were performed in this study and future work is needed to address these issues. All these additional mechanisms could explain the decreased protein amount observed under depleted *hnRNPA0* levels (Fig. S3). A possible influence of *hnRNPA0* on the expression of host immune factors, including interferons and cytokines, affecting the host's ability to control HIV-1 infection, was not analyzed. The regulation of *hnRNPA0* mRNA levels needs to be further analyzed in the context of different cell types, in particular primary cells. Considering the initial suppression followed by subsequent overexpression observed in Jurkat T cells and MDMs, investigating the temporal expression profile of hnRNPA0 levels associated with HIV-1 pre- and post-infection states across various cell types would be reasonable. Although it is very likely that hnRNPA0 binds the HIV-1 promoter, further studies are needed to prove a direct binding of hnRNPA0 to the 5′ LTR sequence. Additional studies are also required to elucidate the mechanistic role of hnRNPA0 in frameshifting.

MATERIALS AND METHODS

Cloning of hnRNPA0 expression vectors

The FLAG-hnRNPA0 expression vector was initially generated by cloning the CDS of the hnRNPA0 gene from cDNA prepared from isolated total RNA from HEK293T cells into pMiniT 2.0 vector (NEB) using primer pairs MW_1246/MW_1247 and MW_1248/MW_1249 for BamHI/XbaI-mediated restriction cloning into pcDNA3.1(+), respectively. Using the following primers hnRNPA0.Flag.Sfi.F and hnRNPA0.Sfi.R (Table S1), the 5′-Flag-tagged hnRNPA0 was cloned into the Sleeping Beauty vector backbone of pSBTet:GP (AddGene Plasmid # 60495) and verified the complete expression cassette by Sanger sequencing. Since the vector backbone constitutively expresses EGFP, the localization and expression levels of doxycycline-induced hnRNPA0 protein were analyzed in cells (Fig. S10). For the experiment performed in Fig. 4g, a N-terminal V5-tagged hnRNPA0 pcDNA3.1 plasmid was used.

Cell culture and preparation of virus stocks

PBMC isolation procedures, cell culturing, and preparation of virus stocks were performed as described elsewhere (39). THP-1 differentiation (Fig. S11) was initially evaluated by staining CD11b using the CD11b antibody listed in Table 1. For the generation of a stable hnRNPA0 expressing Jurkat cell line, cells were transfected following the protocol of the Nucleofector Kit V (Lonza). After several selection rounds using puromycin, the highest GFP-expressing cells were isolated by FACS.

Infection of Jurkat T cells and modulation of hnRNPA0 protein levels

Jurkat cells were counted and transferred into a 15 mL reaction tube. Sufficient amounts of NL4-3 were added to reach an MOI of 2. In the case of overexpressing hnRNPA, 0 1 µg/mL doxycycline was also added. The suspension was carefully mixed and transferred into cell culture plates. 40 h post-infection, cells were washed and 250 nM AMD3100 (Sigma-Aldrich) and 1 µg/mL doxycycline were added to the fresh media. 72 h post-infection, supernatants were harvested and subjected to further analysis. In hnRNPA0 knockdown experiments, Jurkat cells were infected as described above. 24 h post-infection, cells were washed and 12 µM LNA GapmeRs directed against hnRNPA0 or a non-template control (Table S2) were added to the fresh media. 7 days post-infection, supernatants were harvested and subjected to further analysis.

Transient transfection and siRNA-mediated knockdown

A549-LTR-Luc-PEST reporter cells were generated using the Sleeping Beauty transposase system (47, 117). For the LTR assay, 24 h post-seeding cells were transfected either with siRNA targeting hnRNPA0 or a plasmid encoding hnRNPA0 (pcDNA3.1-FLAG-NLS-hnRNPA0) and a plasmid encoding HIV-1 Tat (SVcTat) (118). Off-target siRNA and an empty vector control (pcDNA3.1) were used as controls. Oligonucleotides used for knockdown are summarized in Table S2. Vero cells used in Fig. 5A were additionally transfected using plasmids harboring different HIV-1 LTRs upstream of a Firefly luciferase, a promoter-lacking but luciferase encoding plasmid was used as control (pTA-Luc). The sequences of the transmitted-founder viruses were isolated from the "Panel of Full-Length Transmitted/Founder (T/F) HIV-1 Infectious Molecular Clones (IMCs) (HRP-11919) obtained through the NIH HIV Reagent Program, NIAID, NIH: Panel of Full-Length Transmitted/Founder (T/F) Human Immunodeficiency Virus Type 1 (HIV-1) Infectious Molecular Clones, HRP-11919, contributed by Dr. John C. Kappes." 24 h (overexpression) or 48 h (knockdown) post-transfection, cells were lysed using Lysis-Juice (PJK) and incubated for 15 min under agitation subjected to a freeze and thaw cycle. Lysates were centrifuged for 10 min at 13,000 rpm using a tabletop centrifuge and transferred into an Immuno 96-MicroWell plate (Nunc). Luciferase assays were performed using the GloMax Discover (Promega) and Beetle-Juice (PJK) or Luciferase Assay System (Promega).

To perform dual-luciferase frameshift assays, HEK293T cells were seeded 24 h prior transfection in 12-well plates. For overexpression experiments, cells were transfected with varying amounts of pcDNA3.1 FLAG NLS hnRNPA0. After 6 h, the cells were transfected with the reporter plasmid pDual-HIV either containing the wild-type frameshift site with Renilla luciferase in the frame and Firefly luciferase in the −1 frame or the mutated frameshift site with both luciferases in the frame. For knockdown experiments, HEK293T cells were seeded in six-well plates, cultured for 24 h, and transfected with 8 nM siRNA targeting either hnRNPA0 or a non-target control siRNA. 48 h later, the cells were transfected with the dual-luciferase reporter plasmid, cultured for 24 h, lysed using passive lysis buffer (Promega), and centrifuged for 10 min at 13,000 rpm 4°C. Lysates were transferred into a white 96-well assay plate. Luciferase reporter assays were performed on the GloMax Discover (Promega) using the Dual Luciferase Reporter Assay System (Promega). Frameshift efficiency was determined by the ratio of Firefly luciferase to Renilla luciferase.

RNA isolation, quantitative and semi-quantitative RT-PCR

The cells were harvested, and a total RNA was isolated using RNeasy Mini or RNeasy 96 QIAcube HT Kit (Qiagen) according to the manufacturer's instructions. Some experiments were performed using cDNA. For cDNA synthesis, the RNA concentration and quality were monitored *via* photometric measurement using NanoDrop2000c (Thermo Scientific). For RT 1 µg, RNA was digested with 2 U of DNase I (NEB). After heat inactivation of the DNase at 70°C for 5 min, cDNA synthesis for infection experiments was performed for 60 min at 50°C and 15 min at 72°C using 200 U SuperScript III Reverse

Transcriptase (Invitrogen), 40 U RNase Inhibitor Human Placenta (NEB), 50 pmol Oligo d(T)23 (NEB), and 10 pmol Deoxynucleotide Triphosphate Mix (Promega). For all other experiments, cDNA synthesis was performed for 60 min at 42°C and 5 min at 80°C using ProtoScript II First Strand cDNA synthesis kit (NEB) according to the manufacturer's instructions. Quantitative RT-PCR analysis was performed using Luna Universal qPCR Master Mix (NEB) and Rotor-Gene Q (Qiagen) or CFX96 Real-Time System (BioRad). Primers used for qPCR are already described elsewhere (38). ACTB or GAPDH were used as loading control for normalization. For qualitative analysis of HIV-1 mRNAs, PCR was performed using GoTaq G2 DNA Polymerase (Promega) according to the manufacturer's instructions. The primer and probes used in this study are shown in Table S1. PCR products were separated on non-denaturing polyacrylamide gels (12%), stained with Midori green Advanced DNA stain (Nippon Genetics), and visualized with ADVANCED Fluorescence and ECL Imager (Intas Science Imaging). Plasma HIV-1 RNA levels were quantified using the RealTime HIV-1 m2000 test system (Abbott) according to the manufacturer instructions.

Detection of cellular and viral RNA, proteins, and HIV-1 infectivity

RNA isolation, quantitative, and semi-quantitative RT-PCR and p24-CA ELISA were performed as described previously (39). Primer sequences are listed in Table S1. P24-CA-ELISA of the viral supernatants analyzed in Fig. 4 was performed following the manufacturer's instructions (Sino Biological SEK11695). Primary antibodies used in this study are listed in Table 1. The workflow to determine viral infectivity using TZM-bl cells is described elsewhere (39, 42).

Subcellular fractionation for analysis of mRNA trafficking

HEK293T cells were seeded into six-well plates and 24 h later transfected with the proviral molecular clone NL4-3 and either a plasmid encoding for FLAG-tagged hnRNPA0 (pcDNA3.1-FLAG-NLS-hnRNPA0) or siRNA directed against hnRNPA0 [s21545 (Thermo Scientific)]. An empty vector (pcDNA3.1) or off-target siRNA (Silencer Select Negative Control #2, Thermo Scientific) were used as controls of the respective experiments. 48 h (overexpression) or 72 h (knockdown) post-transfection, cells were washed using PBS, detached from the plate using Accutase, and transferred into reaction tubes. Accutase was inactivated by the addition of 1 vol DMEM. To remove cell culture media, cells were spun at $300 \times g$ for 5 min at RT. The supernatant was removed, the pellet loosened by flicking, and the reaction tube and the cells were resuspended in 350 µL precooled RLN Buffer [50 mM Tris-HCl pH8, 140 mM NaCl, 1.5 mM $MgCl_2$, and 0.5% (vol/vol) NP-40], followed by a 5-min incubation period on ice. Samples were then fractionated via centrifugation at 4°C for 2 min at $300 \times g$. The supernatant containing the cytoplasmic fraction was transferred into new reaction tubes. Residues of the supernatant were removed from the pellet (containing the nuclear fraction) and 1,000 µL RLT buffer was added to both fractions which were then subjected to RNA isolation. A control plate termed "whole-cell lysates" (WCL) was included for each condition and treated the same way like the fractionation samples, despite not separating the nuclear and cytoplasmic fractions from each other. In the following, the expression levels were initially normalized to the respective control (empty vector or non-template siRNA) and after that normalized to the WCL. Fractionation was validated using PCR amplification and melting curve analysis using appropriate primer pairs amplifying the used housekeeping genes *GAPDH* and *ACTB* (Fig. S12).

Statistical analysis

Differences between the two groups were analyzed by unpaired two-tailed student's or Welch's *t*-test. Multiple group analyses were performed using one- or two-way ANOVA followed by Bonferroni, Dunnett's, or Tukey's post hoc test. Mixed models followed by Dunnett's post hoc tests were used for time-series analysis of multiple groups.

A Kruskal-Wallis test with Dunn's post hoc multiple comparisons test was applied to compare mRNA levels in PBMCs from acutely and chronically HIV-1-infected patients as well as from healthy donors due to violation of the assumptions for a parametric test. The outlier was identified *via* Tukey's range test and excluded from further statistical analysis. If not indicated differently, all experiments were repeated in three independent replicates. Asterisks indicated *P*-values as $*P < 0.05$, $**P < 0.01$, $***P < 0.005$ and $****P < 0.0001$.

AUTHOR AFFILIATIONS

[1]Goethe University Frankfurt, University Hospital, Institute for Medical Virology, Frankfurt, Germany

[2]Institute for Virology, University Hospital Essen, University Duisburg-Essen, Essen, Germany

[3]Institute of Pharmaceutical Biology, Goethe-University, Frankfurt am Main, Hessen, Germany

[4]Department of Medicine, University of Colorado Denver, Aurora, Colorado, USA

[5]Institute for the Research on HIV and AIDS-associated Diseases University Hospital Essen, University Duisburg-Essen, Essen, Germany

[6]Department of Dermatology, HPSTD Outpatient Clinic, University Hospital Essen, University Duisburg-Essen, Essen, Germany

PRESENT ADDRESS

Helene Sertznig, Cold Spring Harbor Laboratory, Cold Spring Harbor, New York, USA

AUTHOR ORCIDs

Fabian Roesmann http://orcid.org/0000-0002-5749-4406
Mario L. Santiago http://orcid.org/0000-0001-7792-2706
Kathrin Sutter http://orcid.org/0000-0001-6397-6551
Marek Widera http://orcid.org/0000-0001-5417-9307

DATA AVAILABILITY

Next-generation sequencing data were deposited at the NCBI Sequence Archive BioProject PRJNA422935. Further inquiries can be directed to the corresponding author.

ETHIC STATEMENT

This study has been approved by the Ethics Committee of the Medical Faculty of the University of Duisburg-Essen (14-6155-BO, 16-7016-BO, and 19-8909-BO). A form of consent was not obtained since the data were analyzed anonymously. The funders had no role in study design, data collection and analysis, decision to publish, or manuscript preparation.

ADDITIONAL FILES

The following material is available online.

Supplemental Material

Supplemental material (JVI00534-24-S0001.pdf). Tables S1 and S2; Fig. S1 to S12.
Table S3 (JVI00534-24-S0002.xlsx). Putative hnRNPA0 binding sites in the HIV-1 NL4-3 genome.

REFERENCES

1. Jia X, Zhao Q, Xiong Y. 2015. HIV suppression by host restriction factors and viral immune evasion. Curr Opin Struct Biol 31:106–114. https://doi.org/10.1016/j.sbi.2015.04.004
2. Inubushi R, Tamaki M, Shimano R, Koyama AH, Akari H, Adachi A. 1998. Functional roles of HIV accessory proteins for viral replication (review). Int J Mol Med 2:429–433. https://doi.org/10.3892/ijmm.2.4.429
3. Fanales-Belasio E, Raimondo M, Suligoi B, Buttò S. 2010. HIV virology and pathogenetic mechanisms of infection: a brief overview. Ann. Ist. Super. Sanità 46:5–14. https://doi.org/10.1590/S0021-25712010000100002
4. Deeks SG, Overbaugh J, Phillips A, Buchbinder S. 2015. HIV infection. Nat Rev Dis Primers 1:15035. https://doi.org/10.1038/nrdp.2015.35
5. Watts JM, Dang KK, Gorelick RJ, Leonard CW, Bess JW, Swanstrom R, Burch CL, Weeks KM. 2009. Architecture and secondary structure of an entire HIV-1 RNA genome. Nature 460:711–716. https://doi.org/10.1038/nature08237
6. Emery A, Swanstrom R. 2021. HIV-1: to splice or not to splice, that is the question. Viruses 13:181. https://doi.org/10.3390/v13020181
7. Sertznig H, Hillebrand F, Erkelenz S, Schaal H, Widera M. 2018. Behind the scenes of HIV-1 replication: alternative splicing as the dependency factor on the quiet. Virology 516:176–188. https://doi.org/10.1016/j.virol.2018.01.011
8. Brakier-Gingras L, Charbonneau J, Butcher SE. 2012. Targeting frameshifting in the human immunodeficiency virus. Expert Opin Ther Targets 16:249–258. https://doi.org/10.1517/14728222.2012.665879
9. Uhlén M, Fagerberg L, Hallström BM, Lindskog C, Oksvold P, Mardinoglu A, Sivertsson Å, Kampf C, Sjöstedt E, Asplund A, et al. 2015. Proteomics. tissue-based map of the human proteome. Science 347:1260419. https://doi.org/10.1126/science.1260419
10. Geuens T, Bouhy D, Timmerman V. 2016. The hnRNP family: insights into their role in health and disease. Hum Genet 135:851–867. https://doi.org/10.1007/s00439-016-1683-5
11. Kaur R, Lal SK. 2020. The multifarious roles of heterogeneous ribonucleoprotein A1 in viral infections. Rev Med Virol 30:e2097. https://doi.org/10.1002/rmv.2097
12. Zheng Y, Jönsson J, Hao C, Shoja Chaghervand S, Cui X, Kajitani N, Gong L, Wu C, Schwartz S. 2020. Heterogeneous nuclear ribonucleoprotein A1 (hnRNP A1) and hnRNP A2 inhibit splicing to human papillomavirus 16 splice site SA409 through a UAG-containing sequence in the E7 coding region. J Virol 94:e01509-20. https://doi.org/10.1128/JVI.01509-20
13. Wang L, Wen M, Cao X. 2019. Nuclear hnRNPA2B1 initiates and amplifies the innate immune response to DNA viruses. Science 365:eaav0758. https://doi.org/10.1126/science.aav0758
14. Wang Y, Zhou J, Du Y. 2014. hnRNP A2/B1 interacts with influenza A viral protein NS1 and inhibits virus replication potentially through suppressing NS1 RNA/protein levels and NS1 mRNA nuclear export. Virology 449:53–61. https://doi.org/10.1016/j.virol.2013.11.009
15. Zhou F, Wan Q, Chen S, Chen Y, Wang PH, Yao X, He ML. 2021. Attenuating innate immunity and facilitating beta-coronavirus infection by Nsp1 of SARS-CoV-2 through specific redistributing hnRNP A2/B1 cellular localization. Signal Transduct Target Ther 6:371. https://doi.org/10.1038/s41392-021-00786-y
16. Chiu LY, Emery A, Jain N, Sugarman A, Kendrick N, Luo L, Ford W, Swanstrom R, Tolbert BS. 2022. Encoded conformational dynamics of the HIV splice site A3 regulatory locus: Implications for differential binding of hnRNP splicing auxiliary factors. J Mol Biol 434:167728. https://doi.org/10.1016/j.jmb.2022.167728
17. Li Z, Zeng W, Ye S, Lv J, Nie A, Zhang B, Sun Y, Han H, He Q. 2018. Cellular hnRNP A1 interacts with nucleocapsid protein of porcine epidemic diarrhea virus and impairs viral replication. Viruses 10:127. https://doi.org/10.3390/v10030127

18. Black DL. 2003. Mechanisms of alternative pre-messenger RNA splicing. Annu Rev Biochem 72:291–336. https://doi.org/10.1146/annurev.biochem.72.121801.161720

19. Jean-Philippe J, Paz S, Caputi M. 2013. hnRNP A1: the Swiss army knife of gene expression. Int J Mol Sci 14:18999–19024. https://doi.org/10.3390/ijms140918999

20. Martinez-Contreras R, Cloutier P, Shkreta L, Fisette JF, Revil T, Chabot B. 2007. hnRNP proteins and splicing control. Adv Exp Med Biol 623:123–147. https://doi.org/10.1007/978-0-387-77374-2_8

21. Matera AG, Wang Z. 2014. A day in the life of the spliceosome. Nat Rev Mol Cell Biol 15:108–121. https://doi.org/10.1038/nrm3742

22. Naji S, Ambrus G, Cimermančič P, Reyes JR, Johnson JR, Filbrandt R, Huber MD, Vesely P, Krogan NJ, Yates JR III, Saphire AC, Gerace L. 2012. Host cell interactome of HIV-1 Rev includes RNA helicases involved in multiple facets of virus production. Molecular & Cellular Proteomics 11:M111. https://doi.org/10.1074/mcp.M111.015313

23. Jarboui MA, Bidoia C, Woods E, Roe B, Wynne K, Elia G, Hall WW, Gautier VW. 2012. Nucleolar protein trafficking in response to HIV-1 tat: rewiring the nucleolus. PLoS One 7:e48702. https://doi.org/10.1371/journal.pone.0048702

24. Chen CY, Shyu AB. 1995. AU-rich elements: characterization and importance in mRNA degradation. Trends Biochem Sci 20:465–470. https://doi.org/10.1016/s0968-0004(00)89102-1

25. Myer VE, Steitz JA. 1995. Isolation and characterization of a novel, low abundance hnRNP protein: A0. RNA 1:171–182.

26. Rousseau S, Morrice N, Peggie M, Campbell DG, Gaestel M, Cohen P. 2002. Inhibition of SAPK2A/P38 prevents hnRNP A0 phosphorylation by MAPKAP-K2 and its interaction with cytokine mRNAs. EMBO J 21:6505–6514. https://doi.org/10.1093/emboj/cdf639

27. Young DJ, Stoddart A, Nakitandwe J, Chen S-C, Qian Z, Downing JR, Le Beau MM. 2014. Knockdown of Hnrnpa0, a del(5Q) gene, alters myeloid cell fate in murine cells through regulation of AU-rich transcripts. Haematologica 99:1032–1040. https://doi.org/10.3324/haematol.2013.098657

28. Hamilton BJ, Burns CM, Nichols RC, Rigby WF. 1997. Modulation of AUUUA response element binding by heterogeneous nuclear ribonucleoprotein A1 in human T lymphocytes. the roles of cytoplasmic location, transcription, and phosphorylation. J Biol Chem 272:28732–28741. https://doi.org/10.1074/jbc.272.45.28732

29. Huelga SC, Vu AQ, Arnold JD, Liang TY, Liu PP, Yan BY, Donohue JP, Shiue L, Hoon S, Brenner S, Ares M, Yeo GW. 2012. Integrative genome-wide analysis reveals cooperative regulation of alternative splicing by hnRNP proteins. Cell Rep 1:167–178. https://doi.org/10.1016/j.celrep.2012.02.001

30. Buratti E, Brindisi A, Giombi M, Tisminetzky S, Ayala YM, Baralle FE. 2005. TDP-43 binds heterogeneous nuclear ribonucleoprotein A/B through its C-terminal tail: an important region for the inhibition of cystic fibrosis transmembrane conductance regulator exon 9 splicing. J Biol Chem 280:37572–37584. https://doi.org/10.1074/jbc.M505557200

31. Hutchison S, LeBel C, Blanchette M, Chabot B. 2002. Distinct sets of adjacent heterogeneous nuclear ribonucleoprotein (hnRNP) A1/A2 binding sites control 5' splice site selection in the hnRNP A1 mRNA precursor. J Biol Chem 277:29745–29752. https://doi.org/10.1074/jbc.M203633200

32. Blanchette M, Green RE, MacArthur S, Brooks AN, Brenner SE, Eisen MB, Rio DC. 2009. Genome-wide analysis of alternative pre-mRNA splicing and RNA-binding specificities of the *Drosophila* hnRNP A/B family members. Mol Cell 33:438–449. https://doi.org/10.1016/j.molcel.2009.01.022

33. Wei C, Peng B, Han Y, Chen WV, Rother J, Tomlinson GE, Boland CR, Chaussabel D, Frazier ML, Amos CI. 2015. Mutations of HNRNPA0 and WIF1 predispose members of a large family to multiple cancers. Fam Cancer 14:297–306. https://doi.org/10.1007/s10689-014-9758-8

34. Katze MG, He Y, Gale M. 2002. Viruses and interferon: a fight for supremacy. Nat Rev Immunol 2:675–687. https://doi.org/10.1038/nri888

35. Lee AJ, Ashkar AA. 2018. The dual nature of type I and type II interferons. Front Immunol 9:2061. https://doi.org/10.3389/fimmu.2018.02061

36. Lavender KJ, Gibbert K, Peterson KE, Van Dis E, Francois S, Woods T, Messer RJ, Gawanbacht A, Müller JA, Münch J, Phillips K, Race B, Harper MS, Guo K, Lee EJ, Trilling M, Hengel H, Piehler J, Verheyen J, Wilson CC, Santiago ML, Hasenkrug KJ, Dittmer U. 2016. Interferon alpha subtype-specific suppression of HIV-1 infection *in vivo*. J Virol 90:6001–6013. https://doi.org/10.1128/JVI.00451-16

37. Sutter K, Dickow J, Dittmer U. 2018. Interferon alpha subtypes in HIV infection. Cytokine Growth Factor Rev 40:13–18. https://doi.org/10.1016/j.cytogfr.2018.02.002

38. Sertznig H, Roesmann F, Wilhelm A, Heininger D, Bleekmann B, Elsner C, Santiago M, Schuhenn J, Karakoese Z, Benatzy Y, Snodgrass R, Esser S, Sutter K, Dittmer U, Widera M. 2022. SRSF1 acts as an IFN-I-regulated cellular dependency factor decisively affecting HIV-1 post-integration steps. Front Immunol 13:935800. https://doi.org/10.3389/fimmu.2022.935800

39. Sertznig H, Roesmann F, Wilhelm A, Heininger D, Bleekmann B, Elsner C, Santiago M, Schuhenn J, Karakoese Z, Benatzy Y, Snodgrass R, Esser S, Sutter K, Dittmer U, Widera M. 2022. SRSF1 acts as an IFN-I-regulated cellular dependency factor decisively affecting HIV-1 post-integration steps. Front Immunol 13:935800. https://doi.org/10.3389/fimmu.2022.935800

40. Dreyfuss G, Matunis MJ, Piñol-Roma S, Burd CG. 1993. hnRNP proteins and the biogenesis of mRNA. Annu Rev Biochem 62:289–321. https://doi.org/10.1146/annurev.bi.62.070193.001445

41. Antonelli G, Scagnolari C, Moschella F, Proietti E. 2015. Twenty-five years of type I interferon-based treatment: a critical analysis of its therapeutic use. Cytokine Growth Factor Rev 26:121–131. https://doi.org/10.1016/j.cytogfr.2014.12.006

42. Widera M, Hillebrand F, Erkelenz S, Vasudevan AAJ, Münk C, Schaal H. 2014. A functional conserved intronic G run in HIV-1 intron 3 is critical to counteract APOBEC3G-mediated host restriction. Retrovirology 11:72. https://doi.org/10.1186/s12977-014-0072-1

43. Victoria S, Temerozo JR, Gobbo L, Pimenta-Inada HK, Bou-Habib DC. 2013. Activation of toll-like receptor 2 increases macrophage resistance to HIV-1 infection. Immunobiology 218:1529–1536. https://doi.org/10.1016/j.imbio.2013.06.006

44. Zhou Y, Wang X, Liu M, Hu Q, Song L, Ye L, Zhou D, Ho W. 2010. A critical function of toll-like receptor-3 in the induction of anti-human immunodeficiency virus activities in macrophages. Immunology 131:40–49. https://doi.org/10.1111/j.1365-2567.2010.03270.x

45. Pietrobon AJ, Yoshikawa FSY, Oliveira LM, Pereira NZ, Matozo T, de Alencar BC, Duarte AJS, Sato MN. 2022. Antiviral response induced by toll-like receptor (TLR) 7/TLR8 activation inhibits human immunodeficiency virus type 1 infection in cord blood macrophages. J Infect Dis 225:510–519. https://doi.org/10.1093/infdis/jiab389

46. Lin C, Kuffour EO, Fuchs NV, Gertzen CGW, Kaiser J, Hirschenberger M, Tang X, Xu HC, Michel O, Tao R, Haase A, Martin U, Kurz T, Drexler I, Görg B, Lang PA, Luedde T, Sparrer KMJ, Gohlke H, König R, Münk C. 2023. Regulation of STING activity in DNA sensing by ISG15 modification. Cell Reports 42:113277. https://doi.org/10.1016/j.celrep.2023.113277

47. Widera M, Wilhelm A, Toptan T, Raffel JM, Kowarz E, Roesmann F, Grözinger F, Siemund AL, Luciano V, Külp M, Reis J, Bracharz S, Pallas C, Ciesek S, Marschalek R. 2021. Generation of a sleeping beauty transposon-based cellular system for rapid and sensitive screening for compounds and cellular factors limiting SARS-CoV-2 replication. Front Microbiol 12:701198. https://doi.org/10.3389/fmicb.2021.701198

48. Rogers S, Wells R, Rechsteiner M. 1986. Amino acid sequences common to rapidly degraded proteins: the PEST hypothesis. Science 234:364–368. https://doi.org/10.1126/science.2876518

49. Purcell DF, Martin MA. 1993. Alternative splicing of human immunodeficiency virus type 1 mRNA modulates viral protein expression, replication, and infectivity. J Virol 67:6365–6378. https://doi.org/10.1128/JVI.67.11.6365-6378.1993

50. Hillebrand F, Ostermann PN, Müller L, Degrandi D, Erkelenz S, Widera M, Pfeffer K, Schaal H. 2019. Gymnotic delivery of LNA mixmers targeting viral SREs induces HIV-1 mRNA degradation. Int J Mol Sci 20:1088. https://doi.org/10.3390/ijms20051088

51. Takaori-Kondo A, Shindo K. 2013. HIV-1 Vif: a guardian of the virus that opens up a new era in the research field of restriction factors. Front Microbiol 4:34. https://doi.org/10.3389/fmicb.2013.00034

52. Wang Y, Qian G, Zhu L, Zhao Z, Liu Y, Han W, Zhang X, Zhang Y, Xiong T, Zeng H, Yu X, Yu X, Zhang X, Xu J, Zou Q, Yan D. 2022. HIV-1 Vif

suppresses antiviral immunity by targeting STING. Cell Mol Immunol 19:108–121. https://doi.org/10.1038/s41423-021-00802-9

53. Miller CM, Akiyama H, Agosto LM, Emery A, Ettinger CR, Swanstrom RI, Henderson AJ, Gummuluru S. 2017. Virion-associated Vpr alleviates a postintegration block to HIV-1 infection of Dendritic cells. J Virol 91:e00051-17. https://doi.org/10.1128/JVI.00051-17

54. Keele BF, Giorgi EE, Salazar-Gonzalez JF, Decker JM, Pham KT, Salazar MG, Sun C, Grayson T, Wang S, Li H, et al. 2008. Identification and characterization of transmitted and early founder virus envelopes in primary HIV-1 infection. Proc Natl Acad Sci U S A 105:7552–7557. https://doi.org/10.1073/pnas.0802203105

55. Salazar-Gonzalez JF, Salazar MG, Keele BF, Learn GH, Giorgi EE, Li H, Decker JM, Wang S, Baalwa J, Kraus MH, et al. 2009. Genetic identity, biological phenotype, and evolutionary pathways of transmitted/founder viruses in acute and early HIV-1 infection. J Exp Med 206:1273–1289. https://doi.org/10.1084/jem.20090378

56. Brenchley JM, Schacker TW, Ruff LE, Price DA, Taylor JH, Beilman GJ, Nguyen PL, Khoruts A, Larson M, Haase AT, Douek DC. 2004. CD4+ T cell depletion during all stages of HIV disease occurs predominantly in the gastrointestinal tract. J Exp Med 200:749–759. https://doi.org/10.1084/jem.20040874

57. Schneider T, Jahn HU, Schmidt W, Riecken EO, Zeitz M, Ullrich R. 1995. Loss of CD4 T lymphocytes in patients infected with human immunodeficiency virus type 1 is more pronounced in the duodenal mucosa than in the peripheral blood. Gut 37:524–529. https://doi.org/10.1136/gut.37.4.524

58. Dillon SM, Guo K, Austin GL, Gianella S, Engen PA, Mutlu EA, Losurdo J, Swanson G, Chakradeo P, Keshavarzian A, Landay AL, Santiago ML, Wilson CC. 2018. A compartmentalized type I interferon response in the gut during chronic HIV-1 infection is associated with immunopathogenesis. AIDS 32:1599–1611. https://doi.org/10.1097/QAD.0000000000001863

59. Ivashkiv LB, Donlin LT. 2014. Regulation of type I interferon responses. Nat Rev Immunol 14:36–49. https://doi.org/10.1038/nri3581

60. Hervas-Stubbs S, Perez-Gracia JL, Rouzaut A, Sanmamed MF, Le Bon A, Melero I. 2011. Direct effects of type I Interferons on cells of the immune system. Clin Cancer Res 17:2619–2627. https://doi.org/10.1158/1078-0432.CCR-10-1114

61. Platanias LC. 2005. Mechanisms of type-I- and type-II-interferon-mediated signalling. Nat Rev Immunol 5:375–386. https://doi.org/10.1038/nri1604

62. Megger DA, Philipp J, Le-Trilling VTK, Sitek B, Trilling M. 2017. Deciphering of the human interferon-regulated proteome by mass spectrometry-based quantitative analysis reveals extent and dynamics of protein induction and repression. Front Immunol 8:1139. https://doi.org/10.3389/fimmu.2017.01139

63. Trilling M, Bellora N, Rutkowski AJ, de Graaf M, Dickinson P, Robertson K, Prazeres da Costa O, Ghazal P, Friedel CC, Albà MM, Dölken L. 2013. Deciphering the modulation of gene expression by type I and II Interferons combining 4sU-tagging, translational arrest and in Silico promoter analysis. Nucleic Acids Res 41:8107–8125. https://doi.org/10.1093/nar/gkt589

64. O'Shea JJ, Schwartz DM, Villarino AV, Gadina M, McInnes IB, Laurence A. 2015. The JAK-STAT pathway: impact on human disease and therapeutic intervention. Annu Rev Med 66:311–328. https://doi.org/10.1146/annurev-med-051113-024537

65. Consortium EP. 2012. An integrated encyclopedia of DNA elements in the human genome. Nature 489:57–74. https://doi.org/10.1038/nature11247

66. Luo Y, Hitz BC, Gabdank I, Hilton JA, Kagda MS, Lam B, Myers Z, Sud P, Jou J, Lin K, Baymuradov UK, Graham K, Litton C, Miyasato SR, Strattan JS, Jolanki O, Lee J-W, Tanaka FY, Adenekan P, O'Neill E, Cherry JM. 2020. New developments on the encyclopedia of DNA elements (ENCODE) data portal. Nucleic Acids Res 48:D882–D889. https://doi.org/10.1093/nar/gkz1062

67. Bampton A, Gittings LM, Fratta P, Lashley T, Gatt A. 2020. The role of hnRNPs in frontotemporal dementia and amyotrophic lateral sclerosis. Acta Neuropathol 140:599–623. https://doi.org/10.1007/s00401-020-02203-0

68. Rossbach O, Hung LH, Schreiner S, Grishina I, Heiner M, Hui J, Bindereif A. 2009. Auto- and cross-regulation of the hnRNP L proteins by alternative splicing. Mol Cell Biol 29:1442–1451. https://doi.org/10.1128/MCB.01689-08

69. Kemmerer K, Fischer S, Weigand JE. 2018. Auto- and cross-regulation of the hnRNPs D and DL. RNA 24:324–331. https://doi.org/10.1261/rna.063420.117

70. Chabot B, LeBel C, Hutchison S, Nasim FH, Simard MJ. 2003. Heterogeneous nuclear ribonucleoprotein particle A/B proteins and the control of alternative splicing of the mammalian heterogeneous nuclear ribonucleoprotein particle A1 pre-mRNA. Prog Mol Subcell Biol 31:59–88. https://doi.org/10.1007/978-3-662-09728-1_3

71. Dassi E. 2017. Handshakes and fights: the regulatory interplay of RNA-binding proteins. Front Mol Biosci 4:67. https://doi.org/10.3389/fmolb.2017.00067

72. Müller-McNicoll M, Rossbach O, Hui J, Medenbach J. 2019. Auto-regulatory feedback by RNA-binding proteins. J Mol Cell Biol 11:930–939. https://doi.org/10.1093/jmcb/mjz043

73. Ronkina N, Menon MB, Schwermann J, Tiedje C, Hitti E, Kotlyarov A, Gaestel M. 2010. MAPKAP Kinases MK2 and MK3 in inflammation: complex regulation of TNF biosynthesis via expression and phosphorylation of tristetraprolin. Biochem Pharmacol 80:1915–1920. https://doi.org/10.1016/j.bcp.2010.06.021

74. Lambert M, Benmoussa A, Diallo I, Ouellet-Boutin K, Dorval V, Majeau N, Joly-Beauparlant C, Droit A, Bergeron A, Têtu B, Fradet Y, Pouliot F, Provost P. 2021. Identification of abundant and functional dodecaRNAs (doRNAs) derived from ribosomal RNA. Int J Mol Sci 22:9757. https://doi.org/10.3390/ijms22189757

75. Dong X, Chen X, Lu D, Diao D, Liu X, Mai S, Feng S, Xiong G. 2022. LncRNA miR205HG hinders HNRNPA0 translation: anti-oncogenic effects in esophageal carcinoma. Mol Oncol 16:795–812. https://doi.org/10.1002/1878-0261.13142

76. Jablonski JA, Caputi M. 2009. Role of cellular RNA processing factors in human immunodeficiency virus type 1 mRNA metabolism, replication, and infectivity. J Virol 83:981–992. https://doi.org/10.1128/JVI.01801-08

77. Paz S, Krainer AR, Caputi M. 2014. HIV-1 transcription is regulated by splicing factor SRSF1. Nucleic Acids Res 42:13812–13823. https://doi.org/10.1093/nar/gku1170

78. Damgaard CK, Kahns S, Lykke-Andersen S, Nielsen AL, Jensen TH, Kjems J. 2008. A 5' splice site enhances the recruitment of basal transcription initiation factors in vivo. Mol Cell 29:271–278. https://doi.org/10.1016/j.molcel.2007.11.035

79. Marchand V, Méreau A, Jacquenet S, Thomas D, Mougin A, Gattoni R, Stévenin J, Branlant C. 2002. A janus splicing regulatory element modulates HIV-1 tat and rev mRNA production by coordination of hnRNP A1 cooperative binding. J Mol Biol 323:629–652. https://doi.org/10.1016/s0022-2836(02)00967-1

80. Damgaard CK, Tange TO, Kjems J. 2002. hnRNP A1 controls HIV-1 mRNA splicing through cooperative binding to intron and exon splicing Silencers in the context of a conserved secondary structure. RNA 8:1401–1415. https://doi.org/10.1017/s1355838202023075

81. Widera M, Erkelenz S, Hillebrand F, Krikoni A, Widera D, Kaisers W, Deenen R, Gombert M, Dellen R, Pfeiffer T, Kaltschmidt B, Münk C, Bosch V, Köhrer K, Schaal H. 2013. An intronic G run within HIV-1 intron 2 is critical for splicing regulation of vif mRNA. J Virol 87:2707–2720. https://doi.org/10.1128/JVI.02755-12

82. Lund N, Milev MP, Wong R, Sanmuganantham T, Woolaway K, Chabot B, Abou Elela S, Mouland AJ, Cochrane A. 2012. Differential effects of hnRNP D/AUF1 Isoforms on HIV-1 gene expression. Nucleic Acids Res 40:3663–3675. https://doi.org/10.1093/nar/gkr1238

83. Cartegni L, Maconi M, Morandi E, Cobianchi F, Riva S, Biamonti G. 1996. hnRNP A1 selectively interacts through its Gly-rich domain with different RNA-binding proteins. J Mol Biol 259:337–348. https://doi.org/10.1006/jmbi.1996.0324

84. Weighardt F, Biamonti G, Riva S. 1996. The roles of heterogeneous nuclear ribonucleoproteins (hnRNP) in RNA metabolism. Bioessays 18:747–756. https://doi.org/10.1002/bies.950180910

85. Pont AR, Sadri N, Hsiao SJ, Smith S, Schneider RJ. 2012. mRNA decay factor AUF1 maintains normal aging, telomere maintenance, and suppression of senescence by activation of telomerase transcription. Mol Cell 47:5–15. https://doi.org/10.1016/j.molcel.2012.04.019

86. Malik AK, Flock KE, Godavarthi CL, Loh HH, Ko JL. 2006. Molecular basis underlying the poly C binding protein 1 as a regulator of the proximal

promoter of mouse mu-opioid receptor gene. Brain Research 1112:33–45. https://doi.org/10.1016/j.brainres.2006.07.019

87. Fukuda A, Nakadai T, Shimada M, Hisatake K. 2009. Heterogeneous nuclear ribonucleoprotein R enhances transcription from the naturally configured c-fos promoter in vitro. Journal of Biological Chemistry 284:23472–23480. https://doi.org/10.1074/jbc.M109.013656

88. Kukalev A, Nord Y, Palmberg C, Bergman T, Percipalle P. 2005. Actin and hnRNP U cooperate for productive transcription by RNA polymerase II. Nat Struct Mol Biol 12:238–244. https://doi.org/10.1038/nsmb904

89. Hay DC, Kemp GD, Dargemont C, Hay RT. 2001. Interaction between hnRNPA1 and Ikappabalpha is required for maximal activation of NF-kappaB-dependent transcription. Molecular and Cellular Biology 21:3482–3490. https://doi.org/10.1128/MCB.21.10.3482-3490.2001

90. Byers SA, Price JP, Cooper JJ, Li Q, Price DH. 2005. HEXIM2, a HEXIM1-related protein, regulates positive transcription elongation factor b through association with 7SK. Journal of Biological Chemistry 280:16360–16367. https://doi.org/10.1074/jbc.M500424200

91. Sedore SC, Byers SA, Biglione S, Price JP, Maury WJ, Price DH. 2007. Manipulation of P-TEFB control machinery by HIV: recruitment of P-TEFB from the large form by tat and binding of HEXIM1 to TAR. Nucleic Acids Res 35:4347–4358. https://doi.org/10.1093/nar/gkm443

92. Van Herreweghe E, Egloff S, Goiffon I, Jády BE, Froment C, Monsarrat B, Kiss T. 2007. Dynamic remodelling of human 7SK snRNP controls the nuclear level of active P-TEFB. EMBO J 26:3570–3580. https://doi.org/10.1038/sj.emboj.7601783

93. Barrandon C, Bonnet F, Nguyen VT, Labas V, Bensaude O. 2007. The transcription-dependent dissociation of P-TEFB-HEXIM1-7SK RNA relies upon formation of hnRNP-7SK RNA complexes. Mol Cell Biol 27:6996–7006. https://doi.org/10.1128/MCB.00975-07

94. Lau JS, Baumeister P, Kim E, Roy B, Hsieh TY, Lai M, Lee AS. 2000. Heterogeneous nuclear ribonucleoproteins as regulators of gene expression through interactions with the human thymidine kinase promoter. J Cell Biochem 79:395–406. https://doi.org/10.1002/1097-4644(20001201)79:3<395::aid-jcb50>3.0.co;2-m

95. Huang P-R, Hung S-C, Wang T-CV. 2010. Telomeric DNA-binding activities of heterogeneous nuclear ribonucleoprotein A3 in vitro and in vivo. Biochim Biophys Acta 1803:1164–1174. https://doi.org/10.1016/j.bbamcr.2010.06.003

96. Michelotti EF, Michelotti GA, Aronsohn AI, Levens D. 1996. Heterogeneous nuclear ribonucleoprotein K is a transcription factor. Mol Cell Biol 16:2350–2360. https://doi.org/10.1128/MCB.16.5.2350

97. Baber JL, Libutti D, Levens D, Tjandra N. 1999. High precision solution structure of the C-terminal KH domain of heterogeneous nuclear ribonucleoprotein K, a c-myc transcription factor. J Mol Biol 289:949–962. https://doi.org/10.1006/jmbi.1999.2818

98. Ostrowski J, Kawata Y, Schullery DS, Denisenko ON, Bomsztyk K. 2003. Transient recruitment of the hnRNP K protein to Inducibly transcribed gene loci. Nucleic Acids Res 31:3954–3962. https://doi.org/10.1093/nar/gkg452

99. Stains JP, Lecanda F, Towler DA, Civitelli R. 2005. Heterogeneous nuclear ribonucleoprotein K represses transcription from a cytosine/thymidine-rich element in the osteocalcin promoter. Biochem J 385:613–623. https://doi.org/10.1042/BJ20040680

100. Fackelmayer FO, Dahm K, Renz A, Ramsperger U, Richter A. 1994. Nucleic-acid-binding properties of hnRNP-U/SAF-A, a nuclear-matrix protein which binds DNA and RNA in vivo and in vitro. Eur J Biochem 221:749–757. https://doi.org/10.1111/j.1432-1033.1994.tb18788.x

101. Bi H, Yang X, Yuan J, Yang F, Xu D, Guo Y, Zhang L, Zhou C, Wang F, Sun S. 2013. H19 inhibits RNA polymerase II-mediated transcription by disrupting the hnRNP U-actin complex. Biochim Biophys Acta 1830:4899–4906. https://doi.org/10.1016/j.bbagen.2013.06.026

102. Han SP, Tang YH, Smith R. 2010. Functional diversity of the hnRNPs: past, present and perspectives. Biochem J 430:379–392. https://doi.org/10.1042/BJ20100396

103. Pollard VW, Michael WM, Nakielny S, Siomi MC, Wang F, Dreyfuss G. 1996. A novel receptor-mediated nuclear protein import pathway. Cell 86:985–994. https://doi.org/10.1016/s0092-8674(00)80173-7

104. Siomi MC, Eder PS, Kataoka N, Wan L, Liu Q, Dreyfuss G. 1997. Transportin-mediated nuclear import of heterogeneous nuclear RNP proteins. J Cell Biol 138:1181–1192. https://doi.org/10.1083/jcb.138.6.1181

105. Shan J, Munro TP, Barbarese E, Carson JH, Smith R. 2003. A molecular mechanism for mRNA trafficking in neuronal dendrites. J Neurosci 23:8859–8866. https://doi.org/10.1523/JNEUROSCI.23-26-08859.2003

106. Lee BJ, Cansizoglu AE, Süel KE, Louis TH, Zhang Z, Chook YM. 2006. Rules for nuclear localization sequence recognition by karyopherin beta 2. Cell 126:543–558. https://doi.org/10.1016/j.cell.2006.05.049

107. Cansizoglu AE, Lee BJ, Zhang ZC, Fontoura BMA, Chook YM. 2007. Structure-based design of a pathway-specific nuclear import inhibitor. Nat Struct Mol Biol 14:452–454. https://doi.org/10.1038/nsmb1229

108. Wolozin B, Ivanov P. 2019. Stress granules and neurodegeneration. Nat Rev Neurosci 20:649–666. https://doi.org/10.1038/s41583-019-0222-5

109. Pollard VW, Malim MH. 1998. The HIV-1 rev protein. Annu Rev Microbiol 52:491–532. https://doi.org/10.1146/annurev.micro.52.1.491

110. Brierley I, Dos Ramos FJ. 2006. Programmed ribosomal frameshifting in HIV-1 and the SARS-CoV. Virus Res 119:29–42. https://doi.org/10.1016/j.virusres.2005.10.008

111. Ofori LO, Hilimire TA, Bennett RP, Brown NW, Smith HC, Miller BL. 2014. High-affinity recognition of HIV-1 frameshift-stimulating RNA alters frameshifting in vitro and interferes with HIV-1 infectivity. J Med Chem 57:723–732. https://doi.org/10.1021/jm401438g

112. Zimmer MM, Kibe A, Rand U, Pekarek L, Ye L, Buck S, Smyth RP, Cicin-Sain L, Caliskan N. 2021. The short isoform of the host antiviral protein ZAP acts as an inhibitor of SARS-CoV-2 programmed ribosomal frameshifting. Nat Commun 12:7193. https://doi.org/10.1038/s41467-021-27431-0

113. Wang X, Xuan Y, Han Y, Ding X, Ye K, Yang F, Gao P, Goff SP, Gao G. 2019. Regulation of HIV-1 gag-pol expression by shiftless, an inhibitor of programmed -1 ribosomal frameshifting. Cell 176:625–635. https://doi.org/10.1016/j.cell.2018.12.030

114. Suzuki Y, Chin W-X, Han Q, Ichiyama K, Lee CH, Eyo ZW, Ebina H, Takahashi H, Takahashi C, Tan BH, Hishiki T, Ohba K, Matsuyama T, Koyanagi Y, Tan Y-J, Sawasaki T, Chu JJH, Vasudevan SG, Sano K, Yamamoto N. 2016. Characterization of RyDEN (C19orf66) as an interferon-stimulated cellular inhibitor against Dengue virus replication. PLoS Pathog 12:e1005357. https://doi.org/10.1371/journal.ppat.1005357

115. Dillon SM, Lee EJ, Kotter CV, Austin GL, Gianella S, Siewe B, Smith DM, Landay AL, McManus MC, Robertson CE, Frank DN, McCarter MD, Wilson CC. 2016. Gut dendritic cell activation links an altered colonic microbiome to mucosal and systemic T-cell activation in untreated HIV-1 infection. Mucosal Immunol 9:24–37. https://doi.org/10.1038/mi.2015.33

116. Haile WB, Gavegnano C, Tao S, Jiang Y, Schinazi RF, Tyor WR. 2016. The Janus kinase inhibitor ruxolitinib reduces HIV replication in human macrophages and ameliorates HIV encephalitis in a murine model. Neurobiol Dis 92:137–143. https://doi.org/10.1016/j.nbd.2016.02.007

117. Kowarz E, Löscher D, Marschalek R. 2015. Optimized sleeping beauty transposons rapidly generate stable transgenic cell lines. Biotechnol J 10:647–653. https://doi.org/10.1002/biot.201400821

118. Schaal H, Pfeiffer P, Klein M, Gehrmann P, Scheid A. 1993. Use of DNA end joining activity of a Xenopus laevis egg extract for construction of deletions and expression vectors for HIV-1 Tat and Rev proteins. Gene 124:275–280. https://doi.org/10.1016/0378-1119(93)90405-r